Tomato Fruit Chromoplasts Behave as Respiratory Bioenergetic Organelles during Ripening[1][W][OPEN]

Marta Renato, Irini Pateraki[2], Albert Boronat*, and Joaquín Azcón-Bieto*

Departaments de Biologia Vegetal (M.R., J.A.-B.) and Bioquímica i Biologia Molecular (I.P., A.B.), Facultat de Biologia, Universitat de Barcelona, 08007 Barcelona, Spain; and Centre de Recerca en Agrigenòmica, Consorci CSIC-IRTA-UAB-UB, Campus Universitat Autònoma de Barcelona, 08193 Bellaterra, Spain (M.R., I.P., A.B.)

ORCID IDs: 0000-0003-1499-2189 (M.R.); 0000-0002-7526-2334 (I.P.); 0000-0002-8040-1861 (A.B.); 0000-0003-4313-1505 (J.A.-B.).

During tomato (*Solanum lycopersicum*) fruit ripening, chloroplasts differentiate into photosynthetically inactive chromoplasts. It was recently reported that tomato chromoplasts can synthesize ATP through a respiratory process called chromorespiration. Here we show that chromoplast oxygen consumption is stimulated by the electron donors NADH and NADPH and is sensitive to octyl gallate (Ogal), a plastidial terminal oxidase inhibitor. The ATP synthesis rate of isolated chromoplasts was dependent on the supply of NAD(P)H and was fully inhibited by Ogal. It was also inhibited by the proton uncoupler carbonylcyanide *m*-chlorophenylhydrazone, suggesting the involvement of a chemiosmotic gradient. In addition, ATP synthesis was sensitive to 2,5-dibromo-3-methyl-6-isopropyl-*p*-benzoquinone, a cytochrome b_6f complex inhibitor. The possible participation of this complex in chromorespiration was supported by the detection of one of its components (cytochrome *f*) in chromoplasts using immunoblot and immunocytochemical techniques. The observed increased expression of cytochrome c_6 during ripening suggests that it could act as electron acceptor of the cytochrome b_6f complex in chromorespiration. The effects of Ogal on respiration and ATP levels were also studied in tissue samples. Oxygen uptake of mature green fruit and leaf tissues was not affected by Ogal, but was inhibited increasingly in fruit pericarp throughout ripening (up to 26% in red fruit). Similarly, Ogal caused a significant decrease in ATP content of red fruit pericarp. The number of energized mitochondria, as determined by confocal microscopy, strongly decreased in fruit tissue during ripening. Therefore, the contribution of chromoplasts to total fruit respiration appears to increase in late ripening stages.

Chromoplasts are plastids specialized in the production and accumulation of carotenoids, conferring color to many fruits and flowers. During tomato (*Solanum lycopersicum*) fruit ripening, chloroplasts differentiate into chromoplasts in a process that involves the dismantling of the photosynthetic apparatus and a massive synthesis and deposition of lycopene (Camara et al., 1995). Chromoplasts show a barely studied respiratory process, first reported for daffodil (*Narcissus pseudonarcissus*) chromoplasts and called chromorespiration, which consists of a membrane-bound redox pathway associated with carotenoid desaturation and results in oxygen uptake activity (Nievelstein et al., 1995). The most likely oxidase involved in this respiratory activity is the plastidial terminal oxidase (PTOX), a plastoquinol oxidase homologous to the mitochondrial alternative oxidase (AOX; Carol et al., 1999; Wu et al., 1999). According to its role in chromorespiration and in carotenoid biosynthesis, the expression of PTOX increases during the ripening process of tomato and bell pepper (*Capsicum annuum*) fruits (Josse et al., 2003), in parallel to chromoplast differentiation. PTOX has been characterized in vitro and it has been reported to be inhibited by pyrogallol analogs, specially by octyl gallate (Ogal; Josse et al., 2000). In vivo, PTOX has been studied mainly in chloroplasts. PTOX not only participates in carotenoid biosynthesis in chloroplasts but is also involved in chlororespiration, an electron transport chain present in thylakoids that shares plastoquinone with the photosynthetic electron transport chain (Carol and Kuntz, 2001; McDonald et al., 2011).

In daffodil chromoplast homogenates (Nievelstein et al., 1995) as well as in isolated tomato fruit chromoplasts (Pateraki et al., 2013), NAD(P)H acts as an electron donor for chromorespiration, indicating the participation of NAD(P)H plastoquinone oxidoreductase activity. Considering that tomato fruit chromoplasts derive from chloroplasts, it is possible that some components of the chromoplastic redox pathway could originate from chlororespiration,

[1] This work was supported by the Spanish Ministerio de Ciencia e Innovación (grant no. BIO2009–09523 to A.B., including European Regional Development Funds), the Spanish Consolider-Ingenio 2010 Program (grant no. CSD2007–00036 Centre de Recerca en Agrigenòmica), and the Generalitat de Catalunya (grant no. 2009SGR0026). M.R. is recipient of a predoctoral fellowship from the Spanish Ministerio de Educación, Cultura y Deporte.

[2] Present address: Department of Plant and Environmental Sciences, Faculty of Science, University of Copenhagen, Thorvaldsensvej 40, 1871 Frederiksberg, Denmark.

* Address correspondence to aboronat@ub.edu and jazcon@ub.edu.

The author responsible for distribution of materials integral to the findings presented in this article in accordance with the policy described in the Instructions for Authors (www.plantphysiol.org) is: Joaquín Azcón-Bieto (jazcon@ub.edu).

M.R., A.B., and J.A.-B. designed the research; M.R. performed the research; I.P. contributed the analytic tools; M.R., I.P., A.B., and J.A.-B. analyzed the data; M.R., A.B., and J.A.-B. wrote the article.

[W] The online version of this article contains Web-only data.

[OPEN] Articles can be viewed online without a subscription.

www.plantphysiol.org/cgi/doi/10.1104/pp.114.243931

 © 2014 American Society of Plant Biologists. All Rights Reserved.

Downloaded from www.plantphysiol.org on November 7, 2014 - Published by www.plant.org
Copyright © 2014 American Society of Plant Biologists. All rights reserved.

such as the NAD(P)H:plastoquinone-reductase complex (NDH), which could act as the electron entrance. However, the enzymes involved in chromorespiration are not well known. It was also reported that the oxygen uptake activity of daffodil chromoplast homogenates was sensitive to the classic uncoupler 2,4-dinitrophenol (Nievelstein et al., 1995), and this observation led to the proposal that chromorespiration could be linked to membrane energization. Morstadt et al. (2002) found that liposomes containing daffodil chromoplast proteins and energized by an acid-base transition were able to produce ATP through a chemiosmotic mechanism, demonstrating that daffodil chromoplasts contain a functional H^+-ATP synthase complex. We recently reported that isolated chromoplasts from tomato fruits can synthesize ATP de novo (Pateraki et al., 2013). This process is dependent on an ATP synthase complex containing an atypical γ-subunit without the regulatory dithiol domain, which may be active using lower proton gradients than those present in the chloroplast (Pateraki et al., 2013). This finding is consistent with proteomic analyses that reveal that several proteins related to electron transport and ATP production are present in chromoplasts of ripe fruits, like ATP synthase, some subunits of the NDH complex, and the cytochrome b_6f complex (Barsan et al., 2012; Wang et al., 2013).

Several anabolic pathways that require ATP and reducing agents are active in ripe fruit chromoplasts, such as synthesis of carotenoids, lipids (glycolipids, phospholipids, and sterols), and the shikimate pathway (Bian et al., 2011; Angaman et al., 2012). On the other hand, the ATP synthesis capacity of mitochondria in ripe fruit is low, because its membrane potential diminishes during ripening as a result of the increasing activity of the mitochondrial uncoupling protein (Almeida et al., 1999; Costa et al., 1999). This fact raised the question of whether chromorespiration could play a significant role in the production of ATP at the last stages of ripening. To our knowledge, the ATP synthesis rates of chromoplasts have not been quantified; therefore, it was uncertain whether the endogenous production could provide ATP in significant amounts to address the energy requirements of the chromoplasts. Moreover, there was no information about the quantitative contribution of chromorespiration to total fruit tissue respiration. This work aimed to deepen the study of the chromorespiratory process in isolated tomato fruit chromoplasts and to analyze the relative participation of this pathway in the overall respiration and ATP levels of fruit pericarp in vivo.

RESULTS

Respiration Studies in Isolated Chromoplasts

Respiratory assays with chromoplasts isolated from red tomatoes (*S. lycopersicum* cv Micro-Tom) were conducted using a liquid-phase oxygen electrode to analyze the effect of different substrates, uncouplers, and inhibitors. The chromoplast basal oxygen uptake rate was strongly stimulated by NADH and, to a lesser extent by NADPH (Figs. 1 and 2; Supplemental Fig. S1). Maximal effects were observed at 1 mM concentration. NAD^+ and $NADP^+$ were respectively added to facilitate the transport and regeneration of the coenzymes, improving the linearity of the traces. The subsequent addition of ADP slightly increased the oxygen uptake rate in the presence of both electron donors (Fig. 1, A and B). The uncoupler carbonylcyanide *m*-chlorophenylhydrazone (CCCP) induced an abrupt increase in oxygen consumption when added in the presence of NADH (Fig. 1A), and to a lesser degree when added in the presence of NADPH (Fig. 1B). This is the typical response to uncouplers in respiratory membranes because of the dissipation of the proton gradient and the loss of respiratory control (Terada, 1990). Interestingly, CCCP had no effect in chromoplasts broken by sonication (Fig. 1C), indicating the requirement of undisrupted membrane compartments to generate the proton gradient. Finally, Ogal, a known inhibitor of PTOX (Josse et al., 2003), inhibited the oxygen consumption to basal levels in all cases (Fig. 1, A and B; Supplemental Fig. S2). In our assay conditions, the minimal Ogal concentration that produced the maximal inhibitory effect was 3 mM.

To check that the response to NADH was not the result of mitochondrial contamination, the effect of cytochrome *c* oxidase inhibitors was studied. Sodium cyanide and sodium azide were added after NADH, and none of them produced a detectable inhibition of oxygen consumption activity (Fig. 3A; Supplemental Fig. S3). We also assayed some well-known mitochondrial substrates. Not malate, pyruvate, or succinate significantly increased the oxygen uptake rate in chromoplast samples (Fig. 3, B and C). When the uncoupler CCCP and ADP were added thereafter, there was no stimulatory effect (Fig. 3, B and C), again suggesting that mitochondria were not involved in the observed responses to NADH.

ATP Synthesis in Isolated Chromoplasts

The ATP synthesis rate of isolated chromoplasts has been measured using a kinetic assay based on the luminescent luciferine/luciferase reaction (ENLITEN; Promega). All of the assays were done in the presence of 20 μm P^1,P^5-di(adenosine-5′) pentaphosphate (DAPP), an inhibitor of adenylate kinase that does not affect the ATP synthase (Morstadt et al., 2002).

ATP synthesis was monitored in chromoplasts isolated from 'Micro-Tom' fruits using NADH or NADPH as electron donors. The addition of ADP was required for efficient ATP synthesis, and the ATP synthesis rates in the presence of NADH were higher than those obtained when using NADPH (Fig. 4, A and B). Average rates of several of these experiments are shown in Table I. In the presence of ADP, the simultaneous addition of NADH plus NADPH did not result in a higher ATP synthesis rate, whereas rates were negligible in the absence of electron donor (Table I). To confirm the link between chromoplast oxygen uptake activity and the observed ATP synthesis, we performed similar assays in the presence of CCCP and Ogal. Figure 4 shows selected

Downloaded from www.plantphysiol.org on November 7, 2014 - Published by www.plant.org
Copyright © 2014 American Society of Plant Biologists. All rights reserved.

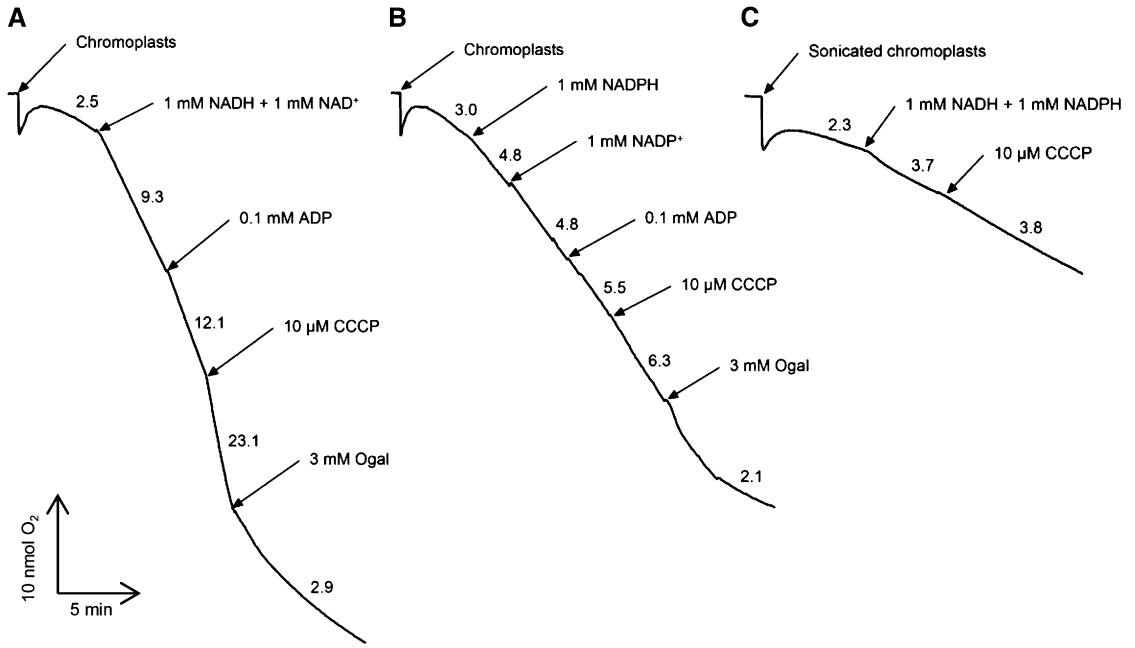

Figure 1. Effect of NAD(P)H on oxygen uptake activity of isolated 'Micro-Tom' fruit chromoplasts. A, Effect of NADH on intact chromoplasts. B, Effect of NADPH on intact chromoplasts. C, Effect of both electron donors on sonicated chromoplasts. Rates are expressed as nmol O_2 mg^{-1} protein min^{-1} and were calculated in the linear zone of the oxygen uptake traces. The addition of ADP, CCCP, Ogal, and their final concentrations in the measurement cuvette are indicated by arrows. The chromoplastic protein content in the electrode cuvette was 0.78 mg (A and B) and 0.50 mg (C). Replicates of these experiments are shown in Supplemental Figure S1.

traces from these assays and average rates of several of these experiments are shown in Supplemental Table S1. CCCP almost completely inhibited the ATP synthesis dependent on NADH and NADPH (Fig. 4, C and D), suggesting that this uncoupler dissipates the proton gradient needed for the activity of ATP synthase. Ogal also inhibited ATP synthesis (Fig. 4, E and F), indicating that this process could be related to PTOX activity. In these experiments, the Ogal minimal concentration that fully inhibited the ATP synthesis (250 μM) was lower than the concentration used in the respiratory assays (Fig. 1).

Furthermore, we assayed diphenylene iodonium (DPI), an inhibitor of flavoenzymes such as NAD(P)H dehydrogenases (O'Donnell et al., 1994). The ATP synthesis was much more sensitive to DPI when NADPH was used as an electron donor instead of NADH (Fig. 5, A and B; Supplemental Table S1), suggesting that two different NAD(P)H dehydrogenases may be involved. We also assayed 2,5-dibromo-3-methyl-6-isopropyl-*p*-benzoquinone (DBMIB), a known inhibitor of the chloroplastic cytochrome b_6f complex that does not affect PTOX (Josse et al., 2003). It decreased the chromoplastic ATP synthesis with both electron donors, indicating that the cytochrome b_6f complex can be active in chromoplasts. Here again, ATP synthesis was most severely affected when using NADPH instead of NADH (Fig. 5, C and D; Supplemental Table S1).

To check whether these responses also occur in chromoplasts of other tomato varieties, equivalent experiments were performed using chromoplasts isolated from 'Ailsa Craig' fruits (*S. lycopersicum* cv Ailsa Craig), a nondwarfed tomato. The ATP synthesis rates obtained in this case, measured on a protein basis, were approximately three times higher than those obtained from

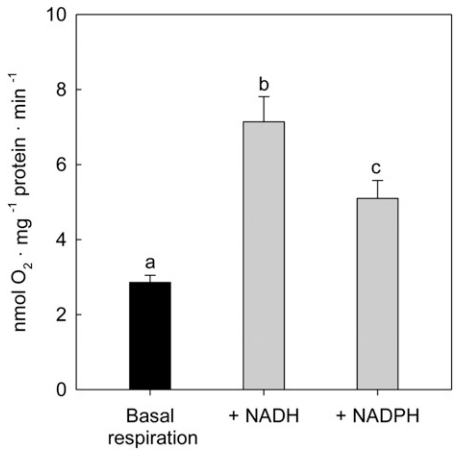

Figure 2. Oxygen uptake rates of isolated 'Micro-Tom' fruit chromoplasts in the absence of substrates (basal respiration) and in the presence of 1 mM NADH (plus 1 mM NAD^+) or 1 mM NADPH (plus 1 mM $NADP^+$). Data are arithmetic means of $n = 30$ for basal respiration, $n = 16$ for NADH, and $n = 14$ for NADPH. Different letters indicate significant differences (Student's t test, $P < 0.05$).

Downloaded from www.plantphysiol.org on November 7, 2014 - Published by www.plant.org
Copyright © 2014 American Society of Plant Biologists. All rights reserved.

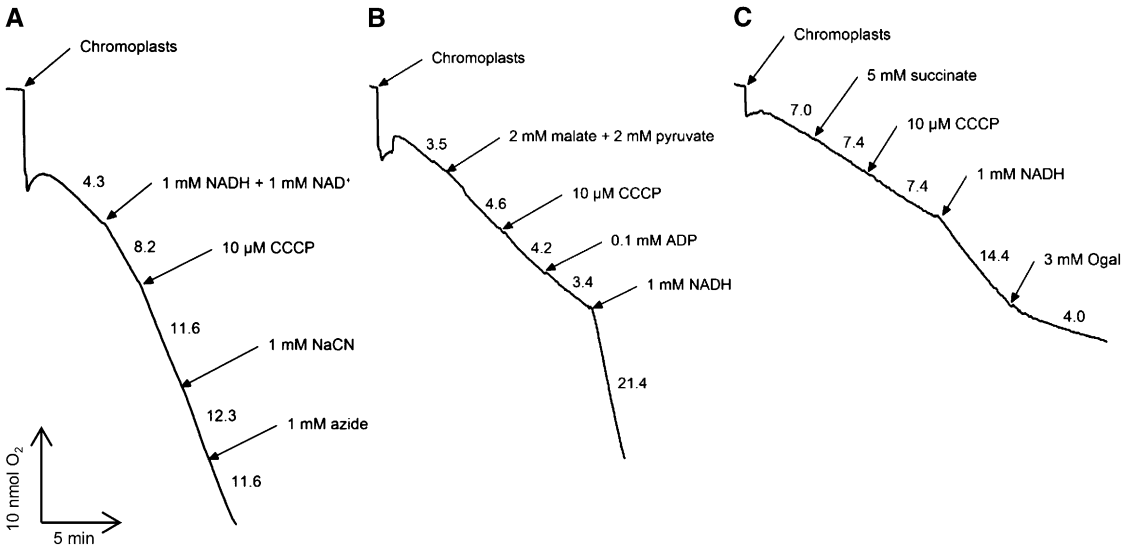

Figure 3. Effect of respiratory substrates and inhibitors on oxygen uptake activity of isolated 'Micro-Tom' chromoplasts. A, Sodium cyanide (NaCN) and sodium azide added after NADH. B, Malate and pyruvate. C, Succinate. Rates are expressed as nmol O_2 mg^{-1} protein min^{-1} and were calculated in the linear zone of the oxygen uptake traces. The addition of other compounds and their final concentrations in the measurement cuvette are indicated by arrows. The chromoplastic protein content in the electrode cuvette was 0.74 mg (A), 0.78 mg (B), and 0.57 mg (C). Replicates of these experiments are shown in Supplemental Figure S3.

'Micro-Tom' chromoplasts (Fig. 6). In 'Ailsa Craig' chromoplasts, the ATP synthesis rates in the presence of NADH were slightly larger than in the presence of NADPH (Fig. 6). With both electron donors, the uncoupler CCCP reduced the ATP synthesis to basal levels and Ogal inhibited it completely. Finally, DBMIB produced an important inhibition only when NADPH was used as an electron donor (Fig. 6). Therefore, these responses are similar to those observed in 'Micro-Tom' chromoplasts.

Immunolocalization of Cytochrome *f* in Chromoplasts

The results reported above suggested that the cytochrome b_6f complex could play an active role in the respiratory process linked to ATP synthesis in chromoplasts. To check this possibility, we performed an immunoblot analysis in chromoplast samples using a polyclonal antibody against cytochrome *f*, a subunit of the cytochrome b_6f complex. A single band with the expected size (32 kD) was detected in leaf protein extract and in chromoplasts isolated from 'Micro-Tom' and 'Ailsa Craig' (Fig. 7A).

The same antibody was used for immunocytochemical analysis of cytochrome *f* in fruit pericarp. Figure 7 shows two electron microscopy images of ripe tomato tissue fixed by the high-pressure freezing method. The presence of elongated membranous sacs and convoluted membranous structures in chromoplasts is easily noted (Fig. 7, B and C). Gold particles were most commonly found adjacent to internal membranes and also in small groups near the carotenoid crystalloids (Fig. 7, B and C), indicating that the cytochrome b_6f complex is found inside chromoplasts.

Expression of Cytochrome c_6

The finding that the cytochrome b_6f complex may participate in chromorespiration led us to try to identify its possible electron acceptor. In the chloroplast, this function is performed by plastocyanin during photosynthesis. However, we were not able to detect plastocyanin in chromoplast samples using immunoblot analysis (results not shown). It has been reported that cyanobacteria present an alternative electron acceptor for the cytochrome b_6f complex, the cytochrome c_6 (Ho et al., 2011), which has a homolog in chloroplasts of higher plants (Gupta et al., 2002; Wastl et al., 2002). To assess the possibility that plastidial cytochrome c_6 may participate in chromorespiration, we analyzed its transcript levels throughout tomato fruit ripening using real-time quantitative PCR. As shown in Figure 8A, the transcript levels of cytochrome c_6 increased during ripening, peaking at orange stage. PTOX expression was also studied (Fig. 8B). Interestingly, the cytochrome c_6 expression profile paralleled that of PTOX, although the changes in PTOX transcript levels were much higher than those of cytochrome c_6.

Effect of Ogal on Total Fruit Tissue Respiration

An important issue is to determine whether the Ogal-sensitive respiratory activity observed in isolated chromoplasts can be a significant component of total fruit tissue respiration. To study this, we analyzed the effect of Ogal upon the oxygen uptake of tomato pericarp throughout ripening (Fig. 9). All measurements were made in darkness in order to avoid interferences with photosynthesis in green tissues. Ogal

Downloaded from www.plantphysiol.org on November 7, 2014 - Published by www.plant.org
Copyright © 2014 American Society of Plant Biologists. All rights reserved.

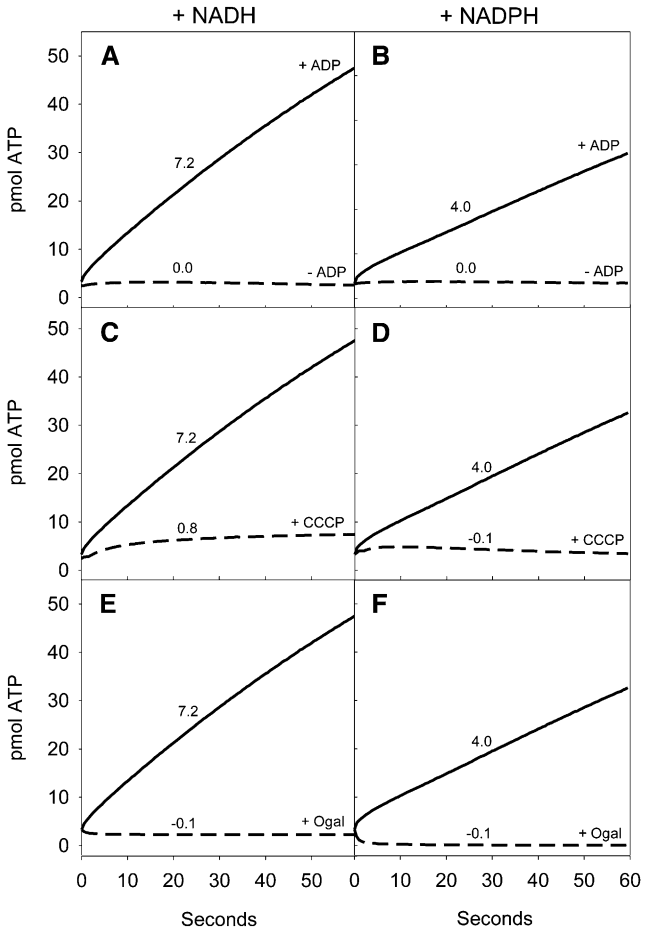

Figure 4. Effect of 0.1 mM ADP (A and B), 10 μM CCCP (C and D), and 250 μM Ogal (E and F) on ATP synthesis activity of isolated 'Micro-Tom' chromoplasts in the presence of NADH or NADPH. ADP was always added in experiments C to F. The reaction well contained 80 μL of buffer ("Materials and Methods"), 80 μL of luciferase/luciferin reagent, 20 μL of chromoplasts (from 0.08–0.14 mg of chromoplastic protein), and 20 μM DAPP. In experiments A, C, and E, 1 mM NADH (plus 1 mM NAD^+) was added. In experiments B, D, and F, 1 mM NADPH (plus 1 mM $NADP^+$) was added. Measurements started after the automatic injection of 0.1 mM ADP at time zero; when ADP was not added, water was injected instead (dashed lines in A and B). Rates on traces are expressed as pmol ATP mg^{-1} protein s^{-1} and were estimated from the slope between 5 and 30 s. The chromoplastic protein concentration in each well was 0.5 mg/ml. Means of three to four assays are shown in Supplemental Table S1.

had no effect at the mature green stage. Inhibition was not statistically significant at the breaker stage, was near 20% at the orange stage, and was approximately 26% at the red stage (Fig. 9). Similarly to the case of mature green fruit, Ogal had no significant effect in 'Micro-Tom' leaves (Fig. 9), indicating that the inhibition produced by Ogal on oxygen uptake is a distinctive feature of the final stages of fruit ripening.

It should be noted that in the oxygen uptake measurements with pericarp tissue, Ogal was used at a 1 mM concentration instead of 3 mM used with isolated chromoplasts (Fig. 1). In other assays using fruit pericarp from a tomato mutant named *ghost*, which lacks functional PTOX (Josse et al., 2000), we observed that 3 mM Ogal produced a slight inhibition of pericarp oxygen uptake (results not shown), suggesting that this inhibitor could be affecting oxidases other than PTOX. Given that Ogal is a quinone analog, it may also inhibit the mitochondrial AOX (Josse et al., 2003) in tissue measurements. However, when Ogal was used at 1 mM concentration, it had no effect in ripe *ghost* fruit respiration, but it strongly decreased oxygen uptake of 'Micro-Tom' red fruit (Supplemental Fig. S4, A and B). These results suggest that Ogal used at 1 mM concentration only affects PTOX. By contrast, salicylhydroxamic acid, which is a stronger inhibitor of AOX, decreased the oxygen uptake rate in pericarp samples of *ghost* and 'Micro-Tom' fruits, suggesting that AOX is active in both fruits (Supplemental Fig. S4, C and D).

In summary, these results indicate that the oxygen uptake related to PTOX activity increases from the mature green stage to the red stage, representing about one-quarter of total pericarp respiration in ripe tomato fruit.

Effect of Ogal on ATP Levels of Tomato Fruit Tissue

To analyze whether chromorespiration could significantly contribute to total ATP synthesis in ripe fruit tissue, we studied the effect of Ogal on ATP content of mature green and red tomato pericarp. Ogal produced a statistically significant decrease in the ATP levels of red pericarp (about 12%), which was not observed in green pericarp (Fig. 10). When pericarp tissue samples were incubated with CCCP, the ATP levels highly decreased in green fruit (83%), whereas the decrease was less pronounced in red fruit (about 47%; Fig. 10). Therefore, the amount of ATP sensitive to CCCP, presumably produced by chemiosmotic mechanisms, is lower in ripe fruit. When the inhibition produced by Ogal in red fruit is referred to the proportion of ATP

Table I. *ATP synthesis rates of isolated 'Micro-Tom' chromoplasts in the presence of ADP, NADH, and/or NADPH*

Measurements were made through a kinetic luminescence assay. The reaction well contained 80 μL of buffer ("Materials and Methods"), 80 μL of luciferase/luciferin reagent, 20 μL of chromoplasts (from 0.08–0.14 mg of chromoplastic protein), 20 μM DAPP and combinations of 0.1 mM of ADP, 1 mM of NADH (plus 1 mM NAD^+), and 1 mM NADPH (plus 1 mM $NADP^+$). Rates are expressed as pmol ATP mg^{-1} protein s^{-1} and were estimated from the slope between 5 and 30 s of the assay. Values are arithmetic means ± SE (n = 3–4). Different letters indicate significant differences (Student's t test, $P < 0.05$).

Addition of ADP	Addition of NADH	Addition of NADPH	ATP Synthesis Rate
			pmol ATP mg^{-1} protein s^{-1}
+	+	−	7.1 ± 0.2^a
−	+	−	0.2 ± 0.1^b
+	−	+	4.7 ± 0.5^c
−	−	+	0 ± 0^b
+	+	+	5.0 ± 0.5^c
+	−	−	-0.7 ± 0.3^d

Downloaded from www.plantphysiol.org on November 7, 2014 - Published by www.plant.org
Copyright © 2014 American Society of Plant Biologists. All rights reserved.

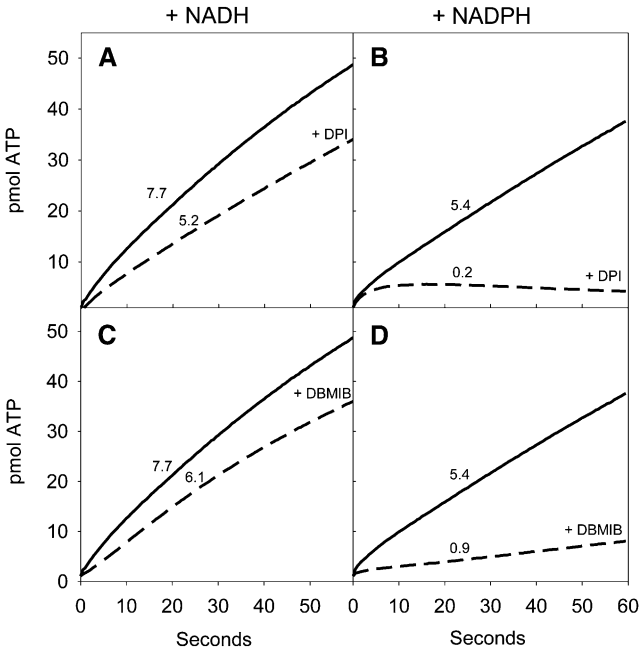

Figure 5. Effect of 50 μM DPI (A and B) and 100 μM DBMIB (C and D) on ATP synthesis activity of isolated 'Micro-Tom' chromoplasts in the presence of NADH or NADPH. The reaction well contained 80 μL of buffer ("Materials and Methods"), 80 μL of luciferase/luciferin reagent, 20 μL of chromoplasts (from 0.08–0.14 mg of chromoplastic protein), and 20 μM DAPP. In experiments A and C, 1 mM NADH (plus 1 mM NAD^+) was added. In experiments B and D, 1 mM NADPH (plus 1 mM $NADP^+$) was added. All of the measurements started after the automatic injection of 0.1 mM ADP at time zero. Rates on traces are expressed as pmol ATP mg^{-1} protein s^{-1} and were estimated from the slope between 5 and 30 s. The chromoplastic protein concentration in each well was 0.5 mg/ml. Means of three to four assays are shown in Supplemental Table S1.

sensitive to CCCP, it results in an inhibition of about 26% of these ATP levels (Fig. 10), a value that is very similar to the inhibition of oxygen uptake produced by Ogal in red pericarp described above (Fig. 9). These data suggest that the ATP synthesis related to PTOX activity may be significant and measurable in ripe fruit.

Quantification of Mitochondria in Tomato Fruit Tissue

Mitochondrial respiration is the major source of ATP in nonphotosynthetic tissues, and we have studied possible changes in the number of mitochondria in tomato fruit pericarp during the ripening process. To this purpose, we made confocal microscopy observations of pericarp slices stained with MitoTracker (Invitrogen), a fluorescent dye that is accumulated only in energized mitochondria holding proton gradients (Jiang et al., 2006). The results shown in Figures 11 and 12, A and B, indicate that the number of stained mitochondria strongly decreased from the mature green stage to the red stage. To confirm the dependence of the staining on the proton gradient, the same observations were done in tissue slices previously incubated with CCCP for 15 min. As shown in Figure 11, the number of energized mitochondria was much lower in all cases.

Interestingly, MitoTracker stained other structures in red fruit pericarp (Fig. 12B), which were identified as chromoplasts by bright-field microscopy (Fig. 12D) and by the autofluorescence of lycopene (Supplemental Fig. S5). By contrast, green fruit chloroplasts (identified by the fluorescence of chlorophyll) were not stained by MitoTracker (Fig. 12A). Considering that tissue fragments were manipulated in darkness during the staining process, a possible explanation is that chloroplastic membranes were probably not energized because they need light to perform these activities, whereas chromoplastic membranes could sustain proton gradients in dark conditions because they are not photosynthetic organelles.

DISCUSSION

We observed that isolated chromoplasts from ripe tomato fruits present a respiratory oxygen uptake activity, which is sensitive to Ogal and is linked to ATP synthesis in the presence of NAD(P)H and ADP. We also found that the cytochrome b_6f complex is present in chromoplasts and is probably involved in chromorespiration. Measurements on pericarp samples have shown

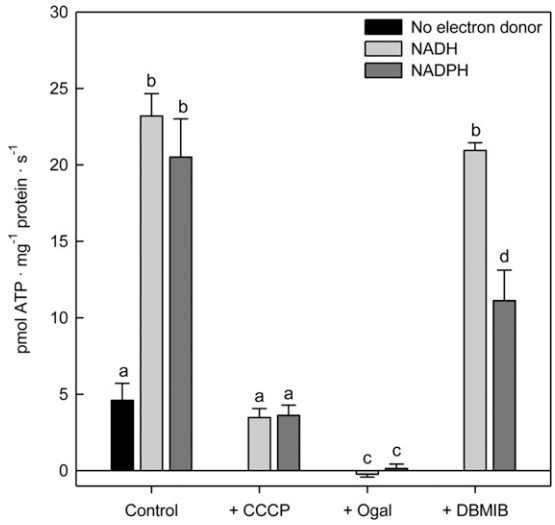

Figure 6. Effect of 10 μM CCCP, 250 μM Ogal, and 100 μM DBMIB on ATP synthesis activity of isolated 'Ailsa Craig' chromoplasts in the presence of NADH or NADPH. The ATP synthesis activity in the absence of any electron donor is also shown. The reaction well contained 80 μL of buffer ("Materials and Methods"), 80 μL of luciferase/luciferin reagent, 20 μL of chromoplasts (from 0.13–0.22 mg of chromoplastic protein), 20 μM DAPP, 0.1 mM of ADP, and 1 mM of NADH (plus 1 mM NAD^+) or 1 mM NADPH (plus 1 mM $NADP^+$). Rates are expressed as pmol ATP mg^{-1} protein s^{-1} and were estimated from the slope between 5 and 30 s of the assays. Data are arithmetic means ± SE (n = 3–4). Different letters indicate significant differences (Student's t test, $P < 0.01$).

Downloaded from www.plantphysiol.org on November 7, 2014 - Published by www.plant.org
Copyright © 2014 American Society of Plant Biologists. All rights reserved.

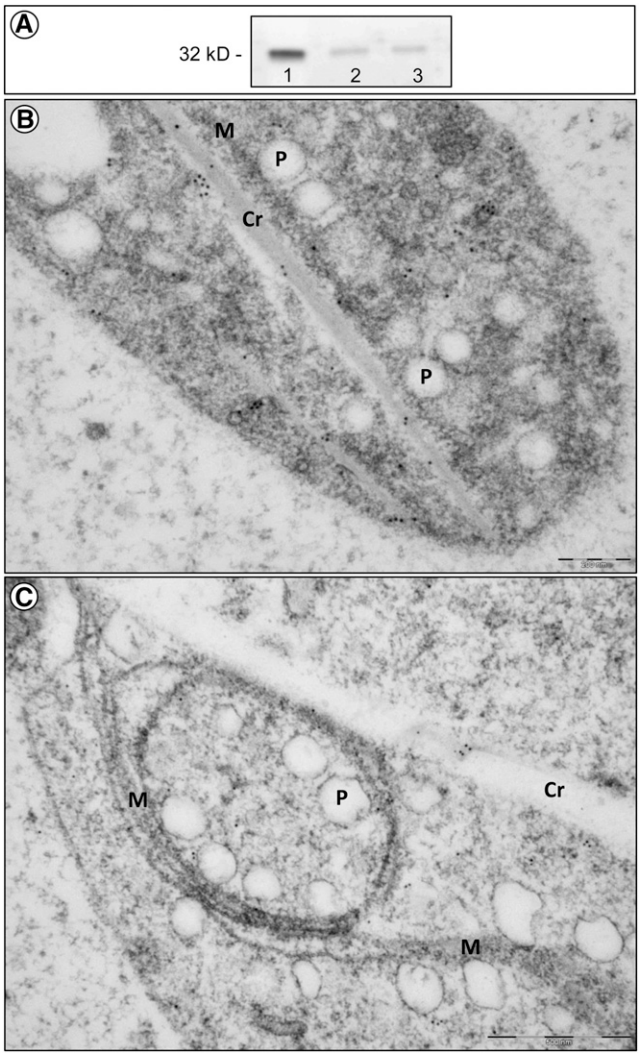

Figure 7. A, Immunoblot analysis of cytochrome *f* in tomato chromoplasts. Western blot of leaf extract of 'Micro-Tom' plants (1) and isolated chromoplast from 'Micro-Tom' fruits (2) and 'Ailsa Craig' fruits (3). A single band of approximately 32 kD was observed. Total protein per lane was 5 μg (1) and 20 μg (2 and 3). This experiment was repeated three times, and a representative immunoblot is shown. B and C, Immunocytochemical analysis of cytochrome *f* in 'Ailsa Craig' red fruit pericarp. The transmission electron micrographs show the ultrastructure of chromoplasts, and gold labeling indicates the presence of the cytochrome *f* protein. Cr, Carotenoid-containing crystalloid; M, chromoplastic internal membranous structures; P, plastoglobule. Bar = 200 nm in B; and 500 nm in C.

that this respiratory activity of chromoplasts may represent about one-quarter of the total oxygen uptake when tomato fruits are ripe, and could also contribute significantly to the total ATP content in red fruit tissue. The progressive increase of chromorespiration during ripening is parallel to the differentiation of chromoplasts; by contrast, the number of energized mitochondria in pericarp tissue was found to sharply decrease from the mature green stage to the red stage. Below we discuss the link between chromorespiration and ATP synthesis, the possible components that participate in this respiratory pathway, and the significance of chromorespiration in the context of fruit ripening.

Chromoplast Respiratory Activity Is Linked to ATP Synthesis

We observed a significant ATP synthesis activity in chromoplasts, which is dependent on ADP plus NADH or NADPH (Figs. 4 and 6). This is consistent with the stimulation of oxygen uptake by NADH and NADPH in isolated chromoplasts (Figs. 1 and 2), and indicates that these reduced dinucleotides act as electron donors in chromorespiration. In both cases, the responses to NADH were usually higher than those observed in the presence of NADPH (Figs. 1, 2, 4, and 6). The ATP synthesis activity was inhibited by CCCP (Figs. 4 and 6), suggesting that a proton gradient generated by chromorespiration could be used to synthesize ATP. This hypothesis is reinforced by the stimulation of oxygen uptake activity observed after the addition of CCCP and ADP (Fig. 1), showing the possible existence of some respiratory control in chromoplasts. Nievelstein et al. (1995) observed a similar respiratory response to NADH, NADPH, and the uncoupler 2,4-dinitrophenol in chromoplasts isolated from daffodil flowers. Pateraki et al., (2013) recently reported the stimulatory effect of NADPH and CCCP on oxygen uptake rates in tomato chromoplasts. Our results are also consistent with the reported existence of an active H^+-ATP synthase in tomato (Pateraki et al., 2013) and daffodil (Morstadt et al., 2002) chromoplasts.

The ATP synthesis activity observed in chromoplasts, as well as the oxygen uptake, were inhibited by Ogal (Figs. 1, 4, and 6), a known inhibitor of PTOX (Josse et al., 2003), indicating that this enzyme is probably the terminal oxidase involved in chromorespiration. Mitochondrial membrane contamination seems to be negligible in view of the lack of effect by inhibitors of cytochrome *c* oxidase (Fig. 3). The assays with marker enzymes performed in our laboratory (Angaman et al., 2012) consistently confirmed the absence of mitochondria and other subcellular organelles in chromoplast samples.

Observation of pericarp slices using transmission electron microscopy revealed the presence of internal membranes in chromoplasts organized in flat or looped layers, which could form compartments holding proton gradients (Fig. 7). The existence of organized internal membranes in tomato chromoplasts was previously reported (Harries and Spurr, 1969; Jeffery et al., 2012) and it is possible that the chromorespiratory pathway may be located in these structures. This hypothesis is in agreement with the lack of effect of CCCP in the respiratory activity of sonicated chromoplasts (Fig. 1), indicating that chromorespiration requires undisrupted membrane compartments.

We quantified the ATP synthesis rates of isolated tomato fruit chromoplasts using a kinetic method (Table I; Fig. 6). Our preliminary work reported that chromoplasts were able to synthesize ATP, although

Downloaded from www.plantphysiol.org on November 7, 2014 - Published by www.plant.org
Copyright © 2014 American Society of Plant Biologists. All rights reserved.

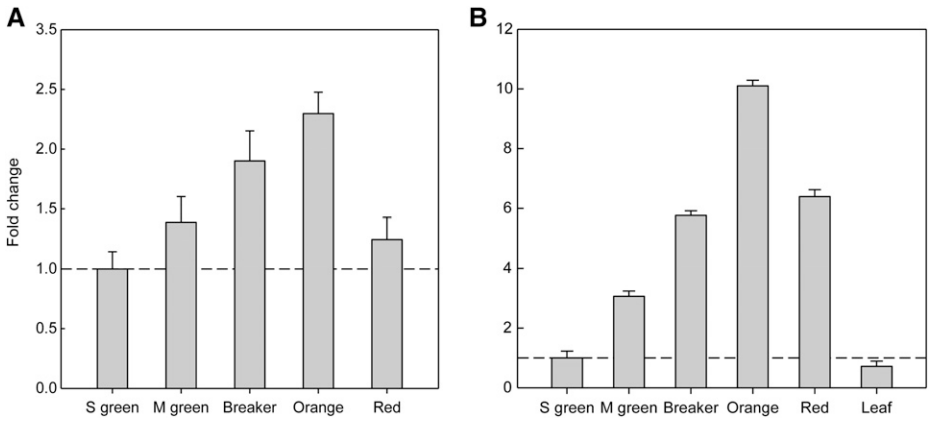

Figure 8. Relative quantification of cytochrome c_6 (A) and PTOX (B) mRNA in different tomato tissues: small green fruit (S green), mature green fruit (M green), breaker fruit, orange fruit, red fruit, and leaf. Data are arithmetic means ± SE of three technical replicates, and experiments were repeated three times (Supplemental Protocol S1). Dashed line indicates the calibrator value (small green fruit).

no attempt to quantify the rates was made (Pateraki et al., 2013). Similarly, Morstadt et al. (2002) measured the ATP synthesis rates of liposomes containing solubilized proteins of daffodil chromoplasts, energized with an acid-base transition. The authors observed a high initial rate of ATP synthesis only maintained for 1 or 2 s, but they did not detect any longer-sustained ATP synthesis in the presence of the adenylate-kinase inhibitor DAPP. By contrast, we observed sustained ATP synthesis for more than 60 s in chromoplasts isolated from two tomato varieties ('Micro-Tom' and 'Ailsa Craig'). However, the ATP synthesis rates of chromoplasts were lower than those measured in wheat (*Triticum durum*) leaf mitochondria when using the same method (Pastore et al., 1996). Unlike mitochondria, chromoplasts are not specialized in ATP export, and thus it is possible that part of the ATP produced could be internally consumed, so the ATP levels detected by our kinetic assay are probably underestimated. Consistently, the plastidial ATP/ADP transporter is expressed at a low level throughout tomato fruit development (Obiadalla-Ali et al., 2004), in agreement with the low ATP transport capacity of chromoplasts.

On the other hand, it is also possible that the proton gradient generated in chromoplasts could be used for purposes other than direct ATP synthesis, such as membrane energization for transport. Regarding this possibility, an active protein translocation mechanism across internal membranes dependent on the change in pH exists in bell pepper chromoplasts, similar to the change in pH-dependent transport found in thylakoids (Summer and Cline, 1999).

Our results suggest that the NADH and the NADPH used by chromoplasts can be imported from the cytosol. Supporting this possibility, the presence of an NAD^+ carrier present in chloroplast envelope was reported in Arabidopsis (*Arabidopsis thaliana*; Palmieri et al., 2009). However, it is also possible that the chromoplast envelopes in our samples presented an increased permeability as a result of the isolation process, thus explaining the instant effect of NADH and NADPH observed on respiration assays. However, the NAD and NADP carriers in the plastid are not well known (Weber and Linka, 2011). In addition, knowledge about changes in envelope permeability and trafficking through plastid differentiation is limited (Fischer, 2011), so further studies are needed to clarify this issue.

Alternatively, NADH and NADPH may be produced inside the chromoplasts. The pentose phosphate pathway generates NADPH and is active in these organelles (Tetlow et al., 2003; Bian et al., 2011). In addition, our previous works proposed the malic enzyme as a source for NADPH in chromoplasts (Angaman et al., 2012; Pateraki et al., 2013), given that they are able to efficiently metabolize malate into pyruvate. Moreover, some plastidic enzymes that use NAD^+ as a cofactor increase its expression in ripe fruit tissue, such as an NAD-dependent malate dehydrogenase and an NAD-specific

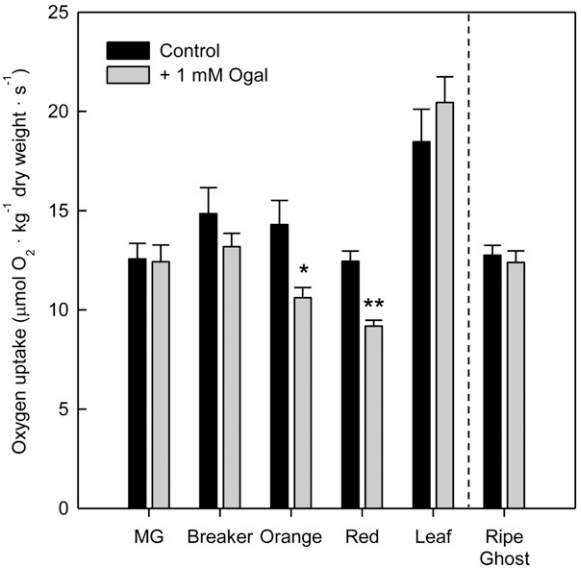

Figure 9. Effect of 1 mM Ogal on oxygen uptake of 'Micro-Tom' fruit pericarp at different ripening stages (mature green, breaker, orange, and red) and 'Micro-Tom' leaf. The effect of Ogal on oxygen uptake of *ghost* ripe fruit pericarp is also shown. Data are arithmetic means ± SE (n = 6–8). Asterisks indicate significant differences from the control (pairwise Student's t test, $^*P < 0.05$ and $^{**}P < 0.01$). MG, Mature green.

Downloaded from www.plantphysiol.org on November 7, 2014 - Published by www.plant.org
Copyright © 2014 American Society of Plant Biologists. All rights reserved.

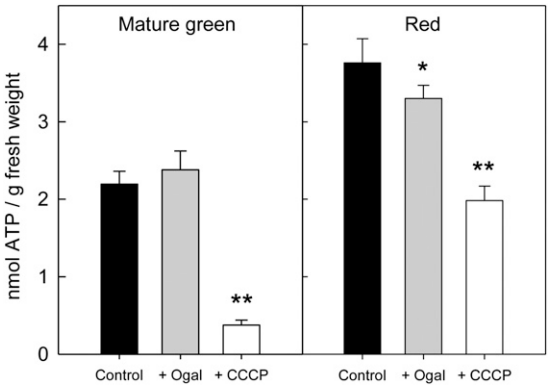

Figure 10. Effect of Ogal and CCCP on the ATP levels of 'Micro-Tom' fruit pericarp at mature green and red stages. Fragments of pericarp were incubated in darkness for 15 min with buffer (control), or buffer supplemented with 1 mM Ogal or 0.1 mM CCCP ("Materials and Methods"). Data are arithmetic means ± SE of duplicate measurements (n = 11–12 different fruits). Asterisks indicate significant differences from the control (pairwise Student's t test, $^*P < 0.05$ and $^{**}P < 0.01$).

glyceraldehyde-3-phosphate dehydrogenase (Backhausen et al., 1998; Petersen et al., 2003), and they may provide NADH for chromorespiration. With the aim of identifying a possible internal source of NADH and NADPH in chromoplasts, we assayed several substrates (e.g. dihydroxyacetone-phosphate, oxaloacetate, malate, Glc, and Glc-6-P) but none of them triggered a stimulation of oxygen uptake (results not shown).

Chromorespiration Involves the Cytochrome b_6f Complex and an NAD(P)H Dehydrogenase

The chromoplastic electron transport chain probably starts with an NAD(P)H dehydrogenase. The most likely plastidic enzyme involved is the NDH complex, homologous to the mitochondrial complex I, which in chloroplasts accepts electrons from NAD(P)H and acts as a proton pump (Peng et al., 2011). In fact, a tomato mutant deficient in one subunit of the plastidial NDH complex accumulates fewer carotenoids and presents changes in antioxidant levels and modifications in fruit shelf-life (Nashilevitz et al., 2010). An alternative electron acceptor in chromoplasts could be the type II NAD(P)H dehydrogenase, a monomeric enzyme that does not act as a proton pump. This type of dehydrogenase is abundant in plant mitochondria and has also been identified in Arabidopsis chloroplasts (Carrie et al., 2008) and in bell pepper chromoplasts (Ytterberg et al., 2006), so it is feasible that it could participate in chromorespiration jointly with the NDH complex. In this work, we assayed DPI, a known inhibitor of type II NAD(P)H dehydrogenase (Mus et al., 2005), although it can also inhibit the mitochondrial complex I and other flavoenzymes (O'Donnell et al., 1994). Given the different effect of DPI on NADH-dependent versus NADPH-dependent ATP synthesis (Fig. 5), there is the possibility that the chromorespiratory electron transport chain could involve two different NAD(P)H dehydrogenases for the electron entrance. Nevertheless, there are no more specific inhibitors available for NDH and type II NAD(P)H dehydrogenase, so further studies based on a molecular approach are needed to clarify this issue.

In a previous work (Pateraki et al., 2013), we proposed the possibility that the cytochrome b_6f complex could be a candidate for the generation of the proton gradient across chromoplast membranes. This complex could accept electrons from NDH or from type II NAD(P)H dehydrogenase through the plastoquinone pool. In this work, we show that the ATP synthesis of chromoplasts is inhibited by the highly specific inhibitor DBMIB (Figs. 5 and 6), suggesting that the cytochrome b_6f complex could participate in chromorespiration. The inhibitor DBMIB shows a similar effect to DPI, because the ATP synthesis is more sensitive when NADPH is used instead of NADH (Figs. 5 and 6). These results raise the possibility that the ATP synthesis activity of chromoplasts could involve a branched electron transport pathway, with one branch accepting electrons from NADH (possibly through NDH) and the other accepting electrons from NADPH (possibly through type II NADPH dehydrogenase), and both converging in PTOX. In this hypothetic model, the cytochrome b_6f complex might act as a proton pump, particularly if type II NADPH dehydrogenase is involved. In our previous work (Pateraki et al., 2013), only the NADPH-dependent pathway was observed.

The participation of the cytochrome b_6f complex in chromorespiration is reinforced by the immunodetection of cytochrome f in chromoplast samples and by its immunocytochemical localization in the internal structures of chromoplasts (Fig. 7). To our knowledge,

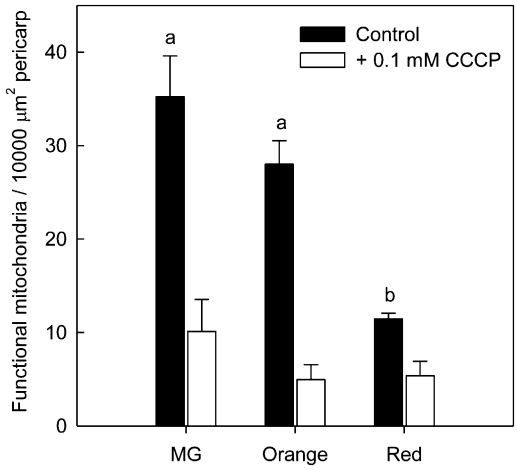

Figure 11. Number of mitochondria stained by MitoTracker (energized mitochondria) per unit area of 'Micro-Tom' fruit pericarp at the mature green, orange, and red ripening stages (black bars). White bars represent the number of stained mitochondria in tissue samples previously incubated with the uncoupler CCCP. Data are arithmetic means ± SE (n = 12 for control and n = 7 for CCCP). Different letters indicate significant differences (Student's t test, $P < 0.01$). MG, Mature green.

Downloaded from www.plantphysiol.org on November 7, 2014 - Published by www.plant.org
Copyright © 2014 American Society of Plant Biologists. All rights reserved.

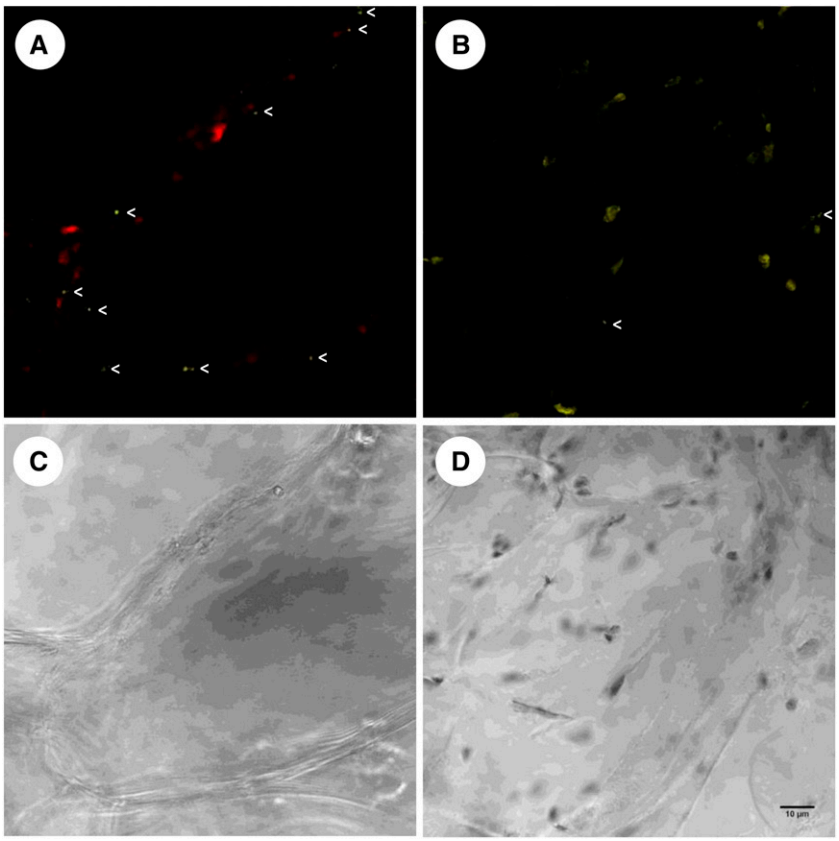

Figure 12. Microscopy images of mature green (A and C) and red (B and D) 'Micro-Tom' fruit pericarp. A and B, Confocal fluorescence images of tissue stained with MitoTracker CM-H_2TMRos (emission, 570–590 nm; in yellow) and overlaid chlorophyll fluorescence (emission, 650–700 nm; in red). C and D, Corresponding bright-field images of A and B. Energized mitochondria are labeled with white arrows. Bar = 10 μm.

this is the first study to show that cytochrome b_6f is related to a nonphotosynthetic function in higher plants.

In the electron transport chain found in thylakoids, the cytochrome b_6f complex receives electrons from plastoquinone and transfers them to plastocyanin. Plastoquinone is certainly present in chromoplasts, where it plays a role as a cofactor in the synthesis of carotenoids (it is required for phytoene desaturation) and it is the substrate of PTOX (Josse et al., 2000). However, we failed in our attempts to reliably detect plastocyanin in isolated chromoplast samples. In cyanobacteria, the photosynthetic and respiratory chains are interconnected inside a single cellular compartment, and the cytochrome b_6f complex can transfer electrons either to plastocyanin or to cytochrome c_6, which is a small soluble redox carrier (Ho et al., 2011). Cytochrome c_6 can then give electrons to PSI during photosynthesis as well as to cytochrome-type oxidases during respiration (Ho et al., 2011). In plants, a plastidic homolog of cytochrome c_6 was identified (Gupta et al., 2002; Wastl et al., 2002). This homolog was named cytochrome c_{6A} and there are different views about its function (for review, see Howe et al., 2006). Our results show that the transcript levels of the plastidic cytochrome c_6 increase during fruit ripening, showing a similar tendency to PTOX expression (Fig. 8). These results are also consistent with the finding (revealed by analysis of complementary DNA libraries) that cytochrome c_6 is expressed in several nonphotosynthetic tissues of higher plants, whereas plastocyanin is restricted to photosynthetic tissues (Wastl et al., 2002). Therefore, the possibility that cytochrome c_6 is involved in chromorespiration exists, but further studies are needed to clarify its role.

All of the results presented above are consistent with recent proteomic studies that have reported that tomato chromoplasts contain high levels of several proteins related to electron transport and ATP synthesis, such as subunits of the complexes cytochrome b_6f, NDH, and ATP synthase (Barsan et al., 2010, 2012; Wang et al., 2013). These components were also identified in chromoplasts generated from nonphotosynthetic plastids, such as those present in oranges (*Citrus sinensis*; Zeng et al., 2011) and carrots (*Daucus carota*; Wang et al., 2013). Therefore, it is unlikely that these electron transport components reported in chromoplasts could be just remnants of chloroplastic proteins with photosynthetic or chlororespiratory functions. In this sense, we recently showed that the ATP synthesis activity in chromoplasts depends on an ATP synthase harboring a γ-subunit that is active in ripe fruit and is differently regulated compared with the chloroplastic subunit (Pateraki et al., 2013). Therefore, we suggest that all of these components could play a specialized role in chromoplasts related to the generation of a proton gradient and the production of ATP in ripe fruit. In conclusion, the obtained results are consistent with the view that chromoplasts may behave as bioenergetic organelles.

Downloaded from www.plantphysiol.org on November 7, 2014 - Published by www.plant.org
Copyright © 2014 American Society of Plant Biologists. All rights reserved.

Chromorespiration Significantly Contributes to Total Pericarp Respiration and ATP Synthesis

The effect of Ogal on tomato pericarp respiration throughout the ripening process (Fig. 9) revealed that the oxygen uptake related to PTOX activity raises from mature green to red fruit, representing up to 26% of total oxygen uptake in ripe tomato. These results are consistent with the increase of PTOX transcript levels during ripening (Fig. 8; Josse et al., 2000).

Until now, it was considered that practically all of the oxygen uptake of fruit was related to mitochondrial metabolism. However, our results using 'Micro-Tom' pericarp samples indicate that chromorespiration could also be an important component of tomato fruit respiration. In addition, we conducted similar assays using pericarp from 'Ailsa Craig' tomato fruits and bell pepper fruits (*Capsicum anuum* cv Yolo Wonder; Supplemental Fig. S6), and we observed that Ogal inhibited about 20% of total oxygen uptake in red fruits but had no effect in green fruits. These responses are similar to those found in 'Micro-Tom' fruits. Such an increase of PTOX activity in both species is in agreement with the enhancement of PTOX transcript levels during fruit ripening reported by Josse et al. (2000) in tomato and bell pepper. Moreover, it should be noted that chromorespiration is not coincident with the climacteric burst of respiration, being that the climacteric burst is measured mainly by CO_2 production and occurs at the onset of color changing (Chalmers and Rowan, 1971), whereas chromoplast respiration appears in later stages of ripening.

Ogal does not inhibit the oxygen uptake rate in tomato leaves or in green fruits (Fig. 9), indicating that this component of respiration is measurable only in tissues containing large amounts of chromoplasts. PTOX is also present in chloroplasts and is involved in chlororespiration, but its expression in green tissues is much lower than in ripening fruit (Fig. 8). The electron flow capacity of PTOX in chloroplasts from tomato leaves is consistently described as being two orders of magnitude lower than the photosynthetic linear flow (Trouillard et al., 2012); therefore, the oxygen uptake activity attributable to PTOX in photosynthetic tissues is probably undetectable by the oxygen electrode.

We also aimed to estimate the contribution of chromoplast ATP synthesis activity to total ATP content in tomato fruit. Our results indicate that the ATP content in green pericarp is lower than in ripe pericarp (Fig. 10), probably because of a higher ATP consumption in green fruit, resulting in a lower ATP accumulation. This result is consistent with the reported increase in ATP levels of tomato pericarp during ripening peaking at the orange stage (Chalmers and Rowan, 1971; Xu et al., 2012). Ripe fruit tissue incubated with Ogal presents a decrease of about 12% in its total ATP content (Fig. 10). By contrast, Ogal does not generate any decrease in ATP levels of green fruit tissue (Fig. 10), indicating that this inhibitor is specifically affecting chromoplast metabolism. These data are consistent with the respiration assays described above, which show that Ogal inhibits about one-quarter of total oxygen uptake in red pericarp, but has no effect in green fruit. Taken together, these results indicate that chromorespiration may significantly contribute to both tissue respiration and ATP synthesis in red fruit.

The proposed bioenergetic role of chromoplasts in ripe fruit is in agreement with the observed decrease in the number of energized mitochondria throughout ripening (Fig. 11). It should be noted, however, that this striking decrease in the number of energized mitochondria is not correlated with the modest decrease observed in total tissue respiration during ripening (Fig. 9). This could be explained by the emergence of chromoplast respiration, and also by the enhanced expression of AOX and the mitochondrial uncoupling protein in ripe fruit (Holtzapffel et al., 2002), which reduce the energization of mitochondria. On the other hand, it is generally accepted that most of the enzymes and intermediates of the Krebs cycle decrease during tomato ripening (Carrari and Fernie, 2006; Carrari et al., 2006; Steinhauser et al., 2010; Biais et al., 2014) as well as the expression of mitochondrial ATP synthase (Holtzapffel et al., 2002). Altogether, data point out that the mitochondrial ATP-generation capacity is low in ripe fruit, again supporting the hypothesis that chromorespiration may play a significant role in the production of ATP at the last stages of ripening.

Chromoplasts are biosynthetically very active because they produce considerable amounts of carotenoids, fatty acids, and other metabolites that are relevant for nutritional and organoleptic fruit quality. To fulfill these tasks, certain levels of energy are required. It is known that in ripe fruits the capacity of mitochondria for ATP synthesis is lower compared with the green ones; moreover, the photosynthetic machinery of the red fruit plastids is degraded. Consequently, it is possible that chromoplasts have developed a light-independent endogenous mechanism for ATP synthesis involving several proteins that participated in the thylakoidal electron transport chain and ATP synthesis, such as the cytochrome b_6f complex, PTOX, NAD(P)H dehydrogenases, and the ATP synthase. Further studies are needed to clarify the relevance of chromorespiration in fruit quality, as well as to identify all of the components involved in this pathway.

MATERIALS AND METHODS

Plant Material

'Micro-Tom' tomato plants (*Solanum lycopersicum* cv Micro-Tom) and bell pepper plants (*Capsicum anuum* cv Yolo Wonder) were maintained in growth chambers with a 16-h-day/8-h-night photoperiod at 250 μmol m^{-2} s^{-1}. Day/night temperatures were set at 22°C/18°C. 'Ailsa Craig' tomato plants were grown in chambers with the same conditions for 4 weeks, and were then maintained in the greenhouse (from September 2013–January 2014). Seeds of the *ghost* mutant, which is impaired in PTOX (Josse et al., 2000), were kindly provided by Marcel Kuntz, and seedlings were maintained in a growth chamber in dim light (40 μmol m^{-2} s^{-1}) for 6 weeks to avoid bleaching. After that period, plants were grown under a light intensity of 100 μmol m^{-2} s^{-1}. The *ghost* mutants had a 16-h-day/8-h-night photoperiod, and the temperature was set at 23°C. All of the plants were watered twice a week with one-half-strength Hoagland solution (Hoagland and Arnon, 1938) and were grown in the University of Barcelona Experimental Fields Service.

Downloaded from www.plantphysiol.org on November 7, 2014 - Published by www.plant.org
Copyright © 2014 American Society of Plant Biologists. All rights reserved.

Chemicals

All of the chemicals used in this study were of the highest grade available and were purchased from Sigma-Aldrich, Panreac, and Calbiochem, unless otherwise stated.

Chromoplast Isolation and Purification

'Micro-Tom' fruits were collected in the red stage (5–7 d after breaker) and processed immediately after harvest. The method for chromoplast isolation was the same as in Angaman et al. (2012), with some modifications. All materials were kept at 4°C during the isolation process. About 300 g of tomato fruits was rinsed with distilled water and the pericarp was cut into small fragments after removing the seeds and the gelatinous material of the locules. The fragments were then mixed with two volumes of isolation buffer (100 mM Tris-HCl, pH 8.2, 330 mM sorbitol, 2 mM $MgCl_2$, 10 mM KCl, 8 mM EDTA, 10 mM sodium ascorbate, 5 mM L-Cys, 1 mM dithiothreitol [DTT], 0.5% [w/v] polyvinylpolypyrrolidone [PVPP], and 0.2% [w/v] bovine serum albumin [BSA]) and homogenized with a blender (Waring Laboratory Science). The homogenate was filtered through two layers of a rayon-polyester filter (Miracloth; Merck Millipore) and centrifuged 10 min at 2000*g*. The obtained pellet was resuspended in 50 mL of isolation buffer without PVPP and centrifuged again 10 min at 2000*g*. The pellet was resuspended in 2 mL of this buffer, layered on a discontinuous gradient (15%, 30%, 40%, and 50% [w/v] of Suc supplemented with 100 mM Tris-HCl, pH 7.4, and 1 mM DTT) and centrifuged at 50,000*g* for 1 h (rotor SW 41 Ti; Beckman). Intact chromoplasts gathered in the 40% to 30% interphase (Angaman et al., 2012) were collected with a pipette, washed with 20 mL of isolation buffer without PVPP, and recovered by centrifugation (2000*g* for 10 min). The pellet was resuspended in the resuspension buffer (100 mM HEPES, 10 mM $MgCl_2$, 2 mM $MnCl_2$, 10 mM KH_2PO_4, 330 mM sorbitol, and 10 μM FAD, pH 7.4). Mitochondrial contamination was excluded considering the undetectable activity of cytochrome *c* oxidase and succinate dehydrogenase observed in respiratory assays (Fig. 3, A and C). The intactness of plastids was analyzed with a fluorescent dye (carboxyfluorescein diacetate), as described in Egea et al. (2010). The observation of plastid suspensions through confocal microscopy revealed that the intactness reached from 60% to 65%.

The total amount of protein of chromoplast samples was measured using the RC DC Protein Assay Kit (Bio-Rad), which is colorimetric assay reducing-agent compatible and detergent compatible. Chromoplast samples were supplemented with Tween 20 (1% [v/v] final concentration), incubated for 30 min at 4°C in agitation, and then processed as recommended by the kit supplier. A typical purification process starting from 200 g of pericarp yielded 7 to 10 mg of total chromoplastic protein.

Respiration Assays with Isolated Chromoplasts

Oxygen uptake was measured in darkness with a liquid-phase oxygen electrode (Qubit Systems; data recording with LoggerPro 3.7 software) using a 1-mL cuvette. For each assay, 0.1 mL of recently isolated chromoplasts was placed in the electrode cuvette containing 0.4 mL of buffer (300 mM sorbitol, 10 mM TES, 2 mM $MgCl_2$, 5 mM KH_2PO_4, and 0.33 mM EDTA, pH 7.4) that was ambient-air equilibrated. The reaction was carried out at 25°C and in constant stirring. All of the reagents were added to the electrode cuvette using a Hamilton syringe. The solvents used were dimethyl sulfoxide (DMSO) for Ogal and CCCP and distilled water for NADH, NADPH, ADP, sodium azide, sodium cyanide, malate, pyruvate, and succinate. For all of the reagents, we applied the minimal concentration that caused the maximum effect, and we checked that the DMSO solvent did not affect the respiratory activity.

ATP Measurements in Isolated Chromoplasts

ATP assays were carried out using a luminometer (Glomax 96 Microplate Luminometer; Promega). To measure the ATP synthesis rates, 20 μL of recently isolated chromoplasts were added to the microplate wells containing 80 μL of luciferase/luciferin reagent (ENLITEN; Promega) and 80 μL of buffer (600 mM sorbitol, 10 mM TES, 2 mM $MgCl_2$, 25 mM KH_2PO_4, and 0.33 mM EDTA, pH 7.4). We checked that the solvent used (DMSO) did not affect the ATP synthesis measurements. The assays started with the automatic injection of ADP, and ATP standards were measured in the same conditions.

Western-Blot Analysis

Fully expanded leaves of 'Micro-Tom' plants were frozen in liquid nitrogen and pulverized in a mortar. Then they were incubated for 15 min at 4°C in a shaker with lysis buffer (0.1 M tricine, 1 mM $MgCl_2$, 10 mM KCl, 10% [w/v] Suc, 1 mM DTT, and 0.2% [v/v] Triton X-100, pH 7.5), supplemented with Complete Protease Inhibitor Cocktail Tablets (Roche Applied Science). The extracts were centrifuged 5 min at 1,000*g* and the supernatant was recovered. Chromoplast samples were incubated for 30 min at 4°C in a shaker with Tween 20 (1% [v/v]). Both leaf extracts and chromoplast samples were mixed with quadruple-strength loading buffer (250 mM Tris-HCl, 8% [w/v] SDS, 40% [v/v] glycerol, 0.02% [w/v] bromophenol blue, and 2 mM DTT, pH 6.8), heated at 95°C for 5 min, and briefly centrifuged to clarify the supernatant.

Western-blot analysis was performed using a polyclonal antibody against cytochrome *f* protein (1:2,500 AS08 306; Agrisera). Proteins were separated by 12.5% denaturing SDS-PAGE, electrotrasferred to polyvinylidene difluoride membrane (Amersham Hybond-P; GE Healthcare) using a wet-electroblotting system (Mini Trans-Blot Cell; Bio-Rad), treated for 1 h at 25°C with blocking buffer (Tris-buffered saline solution supplemented with 5% [w/v] milk powder), and subsequently incubated for 18 h at 4°C with the polyclonal antibody diluted in blocking buffer. The membrane was incubated for 1 h at 25°C with an anti-rabbit horseradish peroxidase-conjugated antibody (1:2,500 A8275; Sigma). Finally, antibody-bound proteins were detected using the Clarity Western ECL substrate (Bio-Rad).

Transmission Electron Microscopy

Fragments of red tomato pericarp were cryoimmobilized by high-pressure freezing using an EM HPM100 device (Leica Microsystems). Freeze substitution of frozen samples was performed in an EM AFS-2 Automatic Freeze Substitution System (Leica Microsystems), using acetone containing 0.5% (w/v) of uranyl acetate, for 3 d at −90°C. On the fourth day, the temperature was slowly increased by 5°C per hour to −50°C. At this temperature, samples were rinsed in acetone and then infiltrated and embedded in Lowicryl HM20 (Polysciences) for 10 d. Ultrathin sections were picked up on Formvar-coated gold grids.

Sections were incubated at room temperature on drops of 5% (w/v) BSA in phosphate-buffered saline (PBS) solution for 20 min, followed by 1:120 anti-cytochrome *f* (AS08 306; Agrisera) in 1% (w/v) BSA in PBS for 2 h. After three washes with drops of 0.25% (v/v) Tween 20 in PBS for 30 min, sections were incubated for 1 h using anti-rabbit coupled to 12-nm diameter colloidal gold particles (British BioCell International) using a 1:40 dilution in 1% (w/v) BSA in PBS. This was followed by three washes with drops of PBS for 5 min, two washes with distilled water, and air-drying. As a control for nonspecific binding of the colloidal gold-conjugated antibody, the primary polyclonal antibody was omitted. Sections were stained with 2% (w/v) uranyl acetate in water and lead citrate, and were observed in a JEM-1010 electron microscope (JEOL) with a SIS Mega View III CCD camera from the Electron Cryomicroscopy Department, at University of Barcelona Scientific and Technological Centers.

Quantitative PCR

mRNA was extracted as described in Bugos et al. (1995). Real-time amplification reactions were conducted in a LightCycler 480 System using SYBR Green I Master (Roche Applied Science). Differences in mRNA abundance of cytochrome c_6 (accession no. XM_004233185) and PTOX (accession no. AF177980) were calculated through normalization with CAC (accession no. XM_00424491), a reference gene stable throughout tomato fruit ripening (Expósito-Rodríguez et al., 2008). A complete description of the methodology used is shown in Supplemental Protocol S1 according to the minimum information for publication of quantitative real-time PCR experiments guidelines (Bustin et al., 2009).

Respiration Assays with Fruit Pericarp and Leaves

'Micro-Tom' tomatoes were collected at the mature green, breaker, orange, and red stages (corresponding to 32, 34, 36, and 41 d after anthesis, respectively). 'Ailsa Craig' tomatoes were collected at the mature green and red stages. *Ghost* tomatoes were collected at the orange stage, which is analogous to the ripe stage of wild-type plants (Barr et al., 2004). Bell pepper fruits were collected at the green (unripe with the same size as ripe fruits) and red (homogeneous red color) stages. Tomato and pepper pericarp was sliced into fragments of about 3 × 3 mm in a $CaCl_2$ solution (0.2 mM) at room temperature (24°C). Fully expanded leaves from 'Micro-Tom' plants were sliced into fragments of 1 × 10 mm in the same conditions. Slices were then infiltrated in respiration buffer (20 mM TES and 2 mM $CaCl_2$, pH 7.2) with a vacuum pump

Downloaded from www.plantphysiol.org on November 7, 2014 - Published by www.plant.org
Copyright © 2014 American Society of Plant Biologists. All rights reserved.

for 30 s. Respiration rates were measured in darkness with the oxygen electrode using a 6-mL cuvette. The tissue was inserted in the electrode cuvette containing 4 mL of respiration buffer, which was ambient-air equilibrated. The reaction was carried out at 25°C and in constant stirring. Inhibitors were dissolved in DMSO and added during the assays using a Hamilton syringe.

ATP Measurements in Pericarp Tissue

'Micro-Tom' fruits were collected at the mature green and red stages and sliced into fragments of 40 to 50 mg. The fragments were incubated for 15 min in darkness at room temperature (24°C) in incubation buffer (50 mM MES and 0.2 mM $CaCl_2$, pH 6.2) supplemented with the corresponding inhibitors, and frozen in liquid nitrogen. Then the extraction and quantification of ATP was carried out through the ATP Bioluminescence Assay Kit HS II (Roche Applied Science) as recommended by the supplier, using a luminometer (Glomax 96 Microplate Luminometer; Promega).

Confocal Microscopy

Pericarp of mature green, orange, and red 'Micro-Tom' fruits was cut with a razor blade into slices of approximately 300-μm thickness, and was incubated in incubation buffer (50 mM MES and 0.2 mM $CaCl_2$, pH 6.2) supplemented with 50 nM of MitoTracker Orange CM-H_2 TMRos (Invitrogen, Molecular Probes) for 30 min at 25°C in darkness. Afterward, the slices were rinsed twice to remove excess MitoTracker. The slices were fixed in incubation buffer supplemented with 3.6% formaldehyde and were observed using a confocal microscope (TCS-SP2; Leica Microsystems) from the University of Barcelona Scientific and Technological Centers (Advanced Optical Microscopy Service, Faculty of Biology). A 63× water immersion objective was used to take the images. Random images of 120 × 120 × 40 μm were analyzed (equivalent to the average size of a pericarp cell) taking one section every 1 μm of thickness, and stained mitochondria were counted in every section using ImageJ software with the PointPicker plug-in.

Supplemental Data

The following materials are available in the online version of this article.

Supplemental Figure S1. Effect of NADH, NADPH, ADP, and CCCP on replicates of oxygen consumption assays of isolated chromoplasts.

Supplemental Figure S2. Effect of Ogal on replicates of oxygen consumption assays of isolated chromoplasts.

Supplemental Figure S3. Effect of respiratory substrates and inhibitors on replicates of oxygen consumption assays of isolated chromoplasts.

Supplemental Figure S4. Effect of Ogal and salicylhydroxamic acid on oxygen uptake of 'Micro-Tom' and *ghost* ripe fruit pericarp.

Supplemental Figure S5. Microscopy images of red tomato fruit pericarp showing the autofluorescence of lycopene.

Supplemental Figure S6. Effect of Ogal on oxygen uptake of 'Ailsa Craig' and bell pepper fruit tissue.

Supplemental Table S1. Effect of CCCP and inhibitors on ATP synthesis rates of isolated chromoplasts in the presence of NADH and NADPH.

Supplemental Protocol S1. Experimental conditions of the quantitative real-time PCR reactions, primer sequences, and data from biological replicates.

ACKNOWLEDGMENTS

We thank Julio Bonilla and Nobahar Panahi (Centre de Recerca en Agrigenòmica) for providing tomato fruit and leaf mRNA; Dr. Manel Bosch Marimon (Advanced Optical Microscopy, University of Barcelona Centres Científics i Tecnològics) and Dr. Carmen López Iglesias (Electron Cryomicroscopy, University of Barcelona Centres Científics i Tecnològics) for technical assistance in microscopy; and Dr. Marcel Kuntz for providing seeds of Ghost mutants.

Received May 28, 2014; accepted August 6, 2014; published August 14, 2014.

LITERATURE CITED

Almeida AM, Jarmuszkiewicz W, Khomsi H, Arruda P, Vercesi AE, Sluse FE (1999) Cyanide-resistant, ATP-synthesis-sustained, and uncoupling-protein-sustained respiration during postharvest ripening of tomato fruit. Plant Physiol **119:** 1323–1330

Angaman DM, Petrizzo R, Hernández-Gras F, Romero-Segura C, Pateraki I, Busquets M, Boronat A (2012) Precursor uptake assays and metabolic analyses in isolated tomato fruit chromoplasts. Plant Methods **8:** 1–10

Backhausen JE, Vetter S, Baalmann E, Kitzmann C, Scheibe R (1998) NAD-dependent malate dehydrogenase and glyceraldehyde 3-phosphate dehydrogenase isoenzymes play an important role in dark metabolism of various plastid types. Planta **205:** 359–366

Barr J, White WS, Chen L, Bae H, Rodermel S (2004) The GHOST terminal oxidase regulates developmental programming in tomato fruit. Plant Cell Environ **27:** 840–852

Barsan C, Sanchez-Bel P, Rombaldi C, Egea I, Rossignol M, Kuntz M, Zouine M, Latché A, Bouzayen M, Pech JC (2010) Characteristics of the tomato chromoplast revealed by proteomic analysis. J Exp Bot **61:** 2413–2431

Barsan C, Zouine M, Maza E, Bian W, Egea I, Rossignol M, Bouyssie D, Pichereaux C, Purgatto E, Bouzayen M, et al (2012) Proteomic analysis of chloroplast-to-chromoplast transition in tomato reveals metabolic shifts coupled with disrupted thylakoid biogenesis machinery and elevated energy-production components. Plant Physiol **160:** 708–725

Biais B, Bénard C, Beauvoit B, Colombié S, Prodhomme D, Ménard G, Bernillon S, Gehl B, Gautier H, Ballias P, et al (2014) Remarkable reproducibility of enzyme activity profiles in tomato fruits grown under contrasting environments provides a roadmap for studies of fruit metabolism. Plant Physiol **164:** 1204–1221

Bian W, Barsan C, Egea I, Purgatto E, Chervin C, Zouine M, Latché A, Bouzayen M, Pech JC (2011) Metabolic and molecular events occurring during chromoplast biogenesis. J Bot **2011:** 1–13

Bugos RC, Chiang VL, Zhang XH, Campbell ER, Podila GK, Campbell WH (1995) RNA isolation from plant tissues recalcitrant to extraction in guanidine. Biotechniques **19:** 734–737

Bustin SA, Benes V, Garson JA, Hellemans J, Huggett J, Kubista M, Mueller R, Nolan T, Pfaffl MW, Shipley GL, et al (2009) The MIQE guidelines: minimum information for publication of quantitative real-time PCR experiments. Clin Chem **55:** 611–622

Camara B, Hugueney P, Bouvier F, Kuntz M, Monéger R (1995) Biochemistry and molecular biology of chromoplast development. Int Rev Cytol **163:** 175–247

Carol P, Kuntz M (2001) A plastid terminal oxidase comes to light: implications for carotenoid biosynthesis and chlororespiration. Trends Plant Sci **6:** 31–36

Carol P, Stevenson D, Bisanz C, Breitenbach J, Sandmann G, Mache R, Coupland G, Kuntz M (1999) Mutations in the *Arabidopsis* gene *IMMUTANS* cause a variegated phenotype by inactivating a chloroplast terminal oxidase associated with phytoene desaturation. Plant Cell **11:** 57–68

Carrari F, Baxter C, Usadel B, Urbanczyk-Wochniak E, Zanor MI, Nunes-Nesi A, Nikiforova V, Centero D, Ratzka A, Pauly M, et al (2006) Integrated analysis of metabolite and transcript levels reveals the metabolic shifts that underlie tomato fruit development and highlight regulatory aspects of metabolic network behavior. Plant Physiol **142:** 1380–1396

Carrari F, Fernie AR (2006) Metabolic regulation underlying tomato fruit development. J Exp Bot **57:** 1883–1897

Carrie C, Murcha MW, Kuehn K, Duncan O, Barthet M, Smith PM, Eubel H, Meyer E, Day DA, Millar AH, et al (2008) Type II NAD(P)H dehydrogenases are targeted to mitochondria and chloroplasts or peroxisomes in *Arabidopsis thaliana*. FEBS Lett **582:** 3073–3079

Chalmers DJ, Rowan KS (1971) The climacteric in ripening tomato fruit. Plant Physiol **48:** 235–240

Costa AD, Nantes IL, Jezek P, Leite A, Arruda P, Vercesi AE (1999) Plant uncoupling mitochondrial protein activity in mitochondria isolated from tomatoes at different stages of ripening. J Bioenerg Biomembr **31:** 527–533

Egea I, Barsan C, Bian W, Purgatto E, Latché A, Chervin C, Bouzayen M, Pech JC (2010) Chromoplast differentiation: current status and perspectives. Plant Cell Physiol **51:** 1601–1611

Expósito-Rodríguez M, Borges AA, Borges-Pérez A, Pérez JA (2008) Selection of internal control genes for quantitative real-time RT-PCR studies during tomato development process. BMC Plant Biol **8:** 131

Downloaded from www.plantphysiol.org on November 7, 2014 - Published by www.plant.org
Copyright © 2014 American Society of Plant Biologists. All rights reserved.

Fischer K (2011) The import and export business in plastids: transport processes across the inner envelope membrane. Plant Physiol **155:** 1511–1519

Gupta R, He Z, Luan S (2002) Functional relationship of cytochrome $c(_6)$ and plastocyanin in *Arabidopsis*. Nature **417:** 567–571

Harries WM, Spurr AR (1969) Chromoplasts of tomato fruit. II. The red tomato. Am J Bot **56:** 380–389

Ho KK, Kerfeld CA, Krogmann DW (2011) The water-soluble cytochromes of cyanobacteria. *In* **Peschek GA, Obinger C, Renger G**, eds, Bioenergetic Processes of Cyanobacteria. Springer Science + Business Media, Dordrecht, Germany, pp 515–540

Hoagland DR, Arnon DI (1938) The water-culture method for growing plants without soil. Univ Calif Agric Exp Stn Circ **347:** 1–3

Holtzapffel RC, Finnegan PM, Millar AH, Badger MR, Day DA (2002) Mitochondrial protein expression in tomato fruit during on-vine ripening and cold storage. Funct Plant Biol **29:** 827–834

Howe CJ, Schlarb-Ridley BG, Wastl J, Purton S, Bendall DS (2006) The novel cytochrome c_6 of chloroplasts: a case of evolutionary bricolage? J Exp Bot **57:** 13–22

Jeffery J, Holzenburg A, King S (2012) Physical barriers to carotenoid bioaccessibility. Ultrastructure survey of chromoplast and cell wall morphology in nine carotenoid-containing fruits and vegetables. J Sci Food Agric **92:** 2594–2602

Jiang K, Ballinger T, Li D, Zhang S, Feldman L (2006) A role for mitochondria in the establishment and maintenance of the maize root quiescent center. Plant Physiol **140:** 1118–1125

Josse EM, Alcaraz JP, Labouré AM, Kuntz M (2003) In vitro characterization of a plastid terminal oxidase (PTOX). Eur J Biochem **270:** 3787–3794

Josse EM, Simkin AJ, Gaffé J, Labouré AM, Kuntz M, Carol P (2000) A plastid terminal oxidase associated with carotenoid desaturation during chromoplast differentiation. Plant Physiol **123:** 1427–1436

McDonald AE, Ivanov AG, Bode R, Maxwell DP, Rodermel SR, Hüner NPA (2011) Flexibility in photosynthetic electron transport: the physiological role of plastoquinol terminal oxidase (PTOX). Biochim Biophys Acta **1807:** 954–967

Morstadt L, Gräber P, De Pascalis L, Kleinig H, Speth V, Beyer P (2002) Chemiosmotic ATP synthesis in photosynthetically inactive chromoplasts from *Narcissus pseudonarcissus* L. linked to a redox pathway potentially also involved in carotene desaturation. Planta **215:** 134–140

Mus F, Cournac L, Cardettini V, Caruana A, Peltier G (2005) Inhibitor studies on non-photochemical plastoquinone reduction and $H(_2)$ photoproduction in *Chlamydomonas reinhardtii.* Biochim Biophys Acta **1708:** 322–332

Nashilevitz S, Melamed-Bessudo C, Izkovich Y, Rogachev I, Osorio S, Itkin M, Adato A, Pankratov I, Hirschberg J, Fernie AR, et al (2010) An orange ripening mutant links plastid NAD(P)H dehydrogenase complex activity to central and specialized metabolism during tomato fruit maturation. Plant Cell **22:** 1977–1997

Nievelstein V, Vandekerchove J, Tadros MH, Lintig JV, Nitschke W, Beyer P (1995) Carotene desaturation is linked to a respiratory redox pathway in *Narcissus pseudonarcissus* chromoplast membranes. Involvement of a 23-kDa oxygen-evolving-complex-like protein. Eur J Biochem **233:** 864–872

O'Donnell VB, Smith GCM, Jones OTG (1994) Involvement of phenyl radicals in iodonium inhibition of flavoenzymes. Mol Pharmacol **46:** 778–785

Obiadalla-Ali H, Fernie AR, Kossmann J, Lloyd JR (2004) Developmental analysis of carbohydrate metabolism in tomato (*Lycopersicon esculentum* cv. Micro-Tom) fruits. Physiol Plant **120:** 196–204

Palmieri F, Rieder B, Ventrella A, Blanco E, Do PT, Nunes-Nesi A, Trauth AU, Fiermonte G, Tjaden J, Agrimi G, et al (2009) Molecular identification and functional characterization of *Arabidopsis thaliana* mitochondrial and chloroplastic NAD^+ carrier proteins. J Biol Chem **284:** 31249–31259

Pastore D, Di Martino C, Bosco G, Passarella S (1996) Stimulation of ATP synthesis via oxidative phosphorylation in wheat mitochondria irradiated with helium-neon laser. Biochem Mol Biol Int **39:** 149–157

Pateraki I, Renato M, Azcón-Bieto J, Boronat A (2013) An ATP synthase harboring an atypical γ-subunit is involved in ATP synthesis in tomato fruit chromoplasts. Plant J **74:** 74–85

Peng L, Yamamoto H, Shikanai T (2011) Structure and biogenesis of the chloroplast NAD(P)H dehydrogenase complex. Biochim Biophys Acta **1807:** 945–953

Petersen J, Brinkmann H, Cerff R (2003) Origin, evolution, and metabolic role of a novel glycolytic GAPDH enzyme recruited by land plant plastids. J Mol Evol **57:** 16–26

Summer EJ, Cline K (1999) Red bell pepper chromoplasts exhibit in vitro import competency and membrane targeting of passenger proteins from the thylakoidal sec and DeltapH pathways but not the chloroplast signal recognition particle pathway. Plant Physiol **119:** 575–584

Steinhauser MC, Steinhauser D, Koehl K, Carrari F, Gibon Y, Fernie AR, Stitt M (2010) Enzyme activity profiles during fruit development in tomato cultivars and *Solanum pennellii.* Plant Physiol **153:** 80–98

Terada H (1990) Uncouplers of oxidative phosphorylation. Environ Health Perspect **87:** 213–218

Tetlow IJ, Bowsher CG, Emes MJ (2003) Biochemical properties and enzymic capacities of chromoplasts isolated from wild buttercup (*Ranunculus acris* L.). Plant Sci **165:** 383–394

Trouillard M, Shahbazi M, Moyet L, Rappaport F, Joliot P, Kuntz M, Finazzi G (2012) Kinetic properties and physiological role of the plastoquinone terminal oxidase (PTOX) in a vascular plant. Biochim Biophys Acta **1817:** 2140–2148

Wang YQ, Yang Y, Fei Z, Yuan H, Fish T, Thannhauser TW, Mazourek M, Kochian LV, Wang X, Li L (2013) Proteomic analysis of chromoplasts from six crop species reveals insights into chromoplast function and development. J Exp Bot **64:** 949–961

Wastl J, Bendall DS, Howe CJ (2002) Higher plants contain a modified cytochrome $c(_6)$. Trends Plant Sci **7:** 244–245

Weber APM, Linka N (2011) Connecting the plastid: transporters of the plastid envelope and their role in linking plastidial with cytosolic metabolism. Annu Rev Plant Biol **62:** 53–77

Wu D, Wright DA, Wetzel C, Voytas DF, Rodermel S (1999) The *IMMUTANS* variegation locus of *Arabidopsis* defines a mitochondrial alternative oxidase homolog that functions during early chloroplast biogenesis. Plant Cell **11:** 43–55

Xu F, Yuan S, Zhang DW, Lv X, Lin HH (2012) The role of alternative oxidase in tomato fruit ripening and its regulatory interaction with ethylene. J Exp Bot **63:** 5705–5716

Ytterberg AJ, Peltier JB, van Wijk KJ (2006) Protein profiling of plastoglobules in chloroplasts and chromoplasts. A surprising site for differential accumulation of metabolic enzymes. Plant Physiol **140:** 984–997

Zeng Y, Pan Z, Ding Y, Zhu A, Cao H, Xu Q, Deng X (2011) A proteomic analysis of the chromoplasts isolated from sweet orange fruits [Citrus sinensis (L.) Osbeck]. J Exp Bot **62:** 5297–5309

Downloaded from www.plantphysiol.org on November 7, 2014 - Published by www.plant.org
Copyright © 2014 American Society of Plant Biologists. All rights reserved.

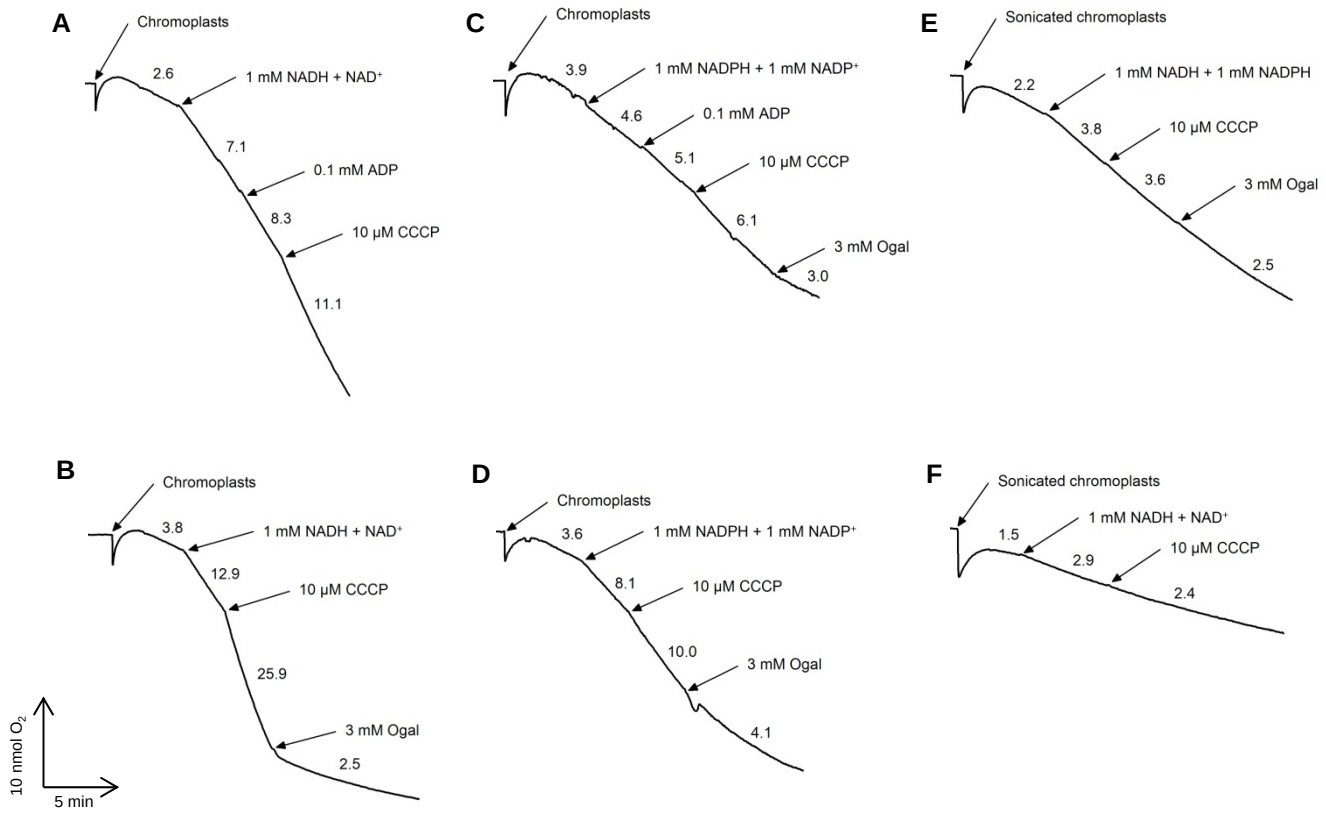

Figure S1. Effect of NAD(P)H on oxygen uptake activity of isolated Micro-Tom fruit chromoplasts. A and B: Effect of NADH on intact chromoplasts. C and D: Effect of NADPH on intact chromoplasts. E and F: Effect of both electron donors on sonicated chromoplasts. Rates are expressed as nmol O_2 mg^{-1} protein min^{-1} and were calculated in the linear zone of the oxygen uptake traces. The addition of ADP, CCCP, octyl gallate (Ogal) and their final concentrations in the measurement cuvette are indicated by arrows. The chromoplastic protein content in the electrode cuvette was 0.68 mg (A), 0.40 mg (B), 0.57 mg (C), 0.47 mg (D), 0.82 mg (E) and 0.43 mg (F).

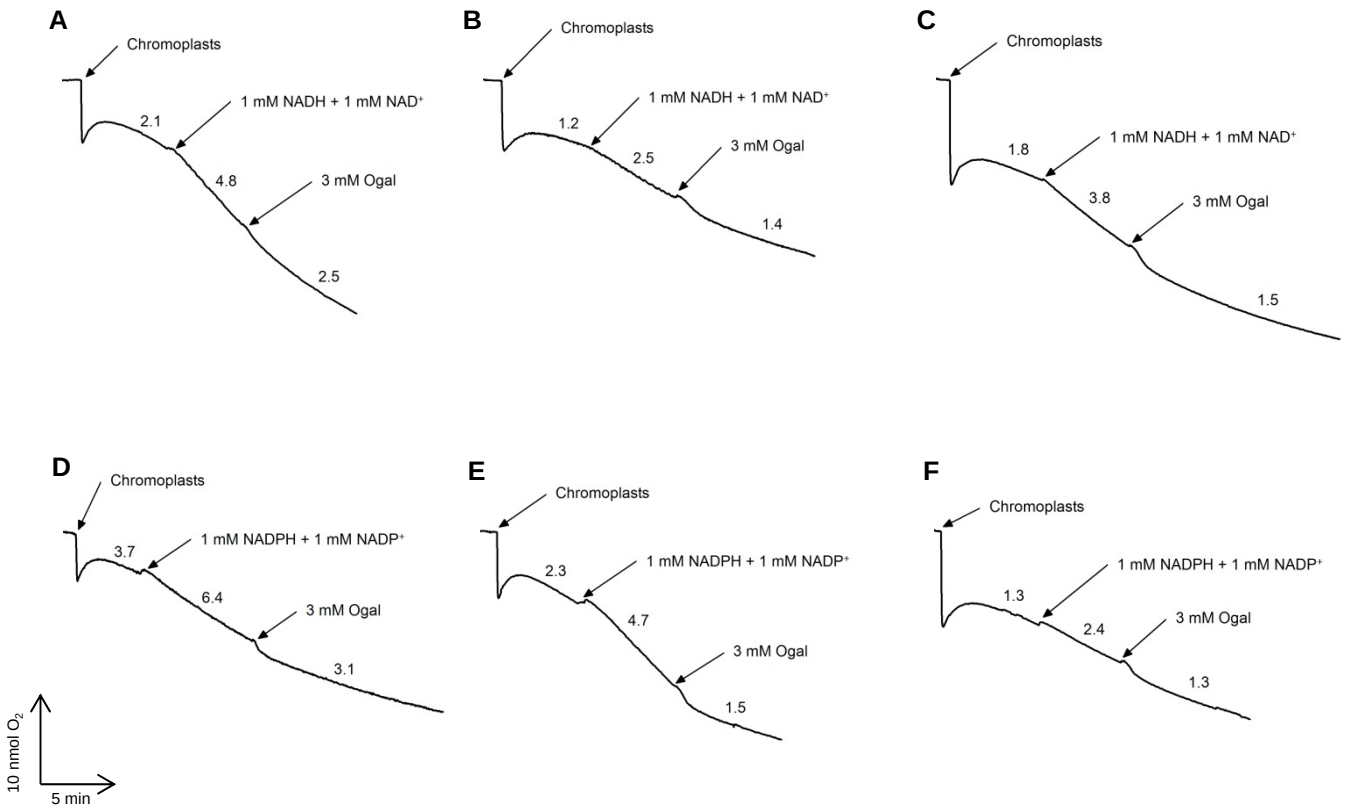

Figure S2. Effect of octyl gallate (Ogal) on oxygen uptake activity of isolated "Micro-Tom" fruit chromoplasts in the presence of NADH (A, B and C) or NADPH (D, E and F). Rates are expressed as nmol O_2 mg^{-1} protein min^{-1} and were calculated in the linear zone of the oxygen uptake traces. The addition of other compounds and their final concentrations in the measurement cuvette are indicated by arrows. The chromoplastic protein content in the electrode cuvette was 0.81 mg (A), 0.97 mg (B), 0.87 mg (C), 0.37 mg (D), 0.87 mg (E) and 0.97 mg (F).

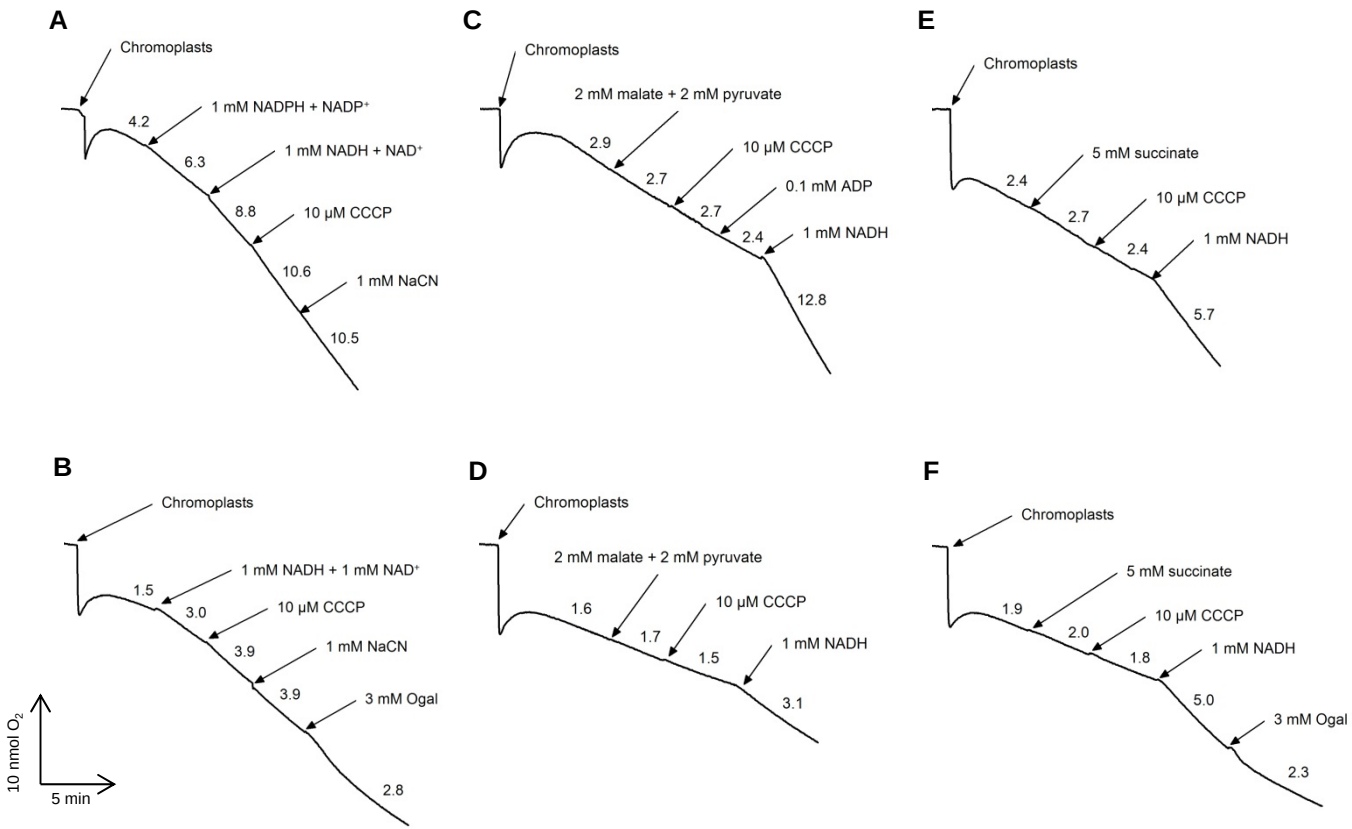

Figure S3. Effect of respiratory substrates and inhibitors on oxygen uptake activity of isolated “Micro-Tom” fruit chromoplasts. A and B: Sodium cyanide (NaCN) added after NADH. C and D: Malate and pyruvate. E and F: Succinate. Rates are expressed as nmol O_2 mg^{-1} protein min^{-1} and were calculated in the linear zone of the oxygen uptake traces. The addition of other compounds and their final concentrations in the measurement cuvette are indicated by arrows. The chromoplastic protein content in the electrode cuvette was 0.44 mg (A), 0.95 mg (B), 0.81 mg (C), 0.97 mg (D), 0.81 mg (E) and 0.87 mg (F).

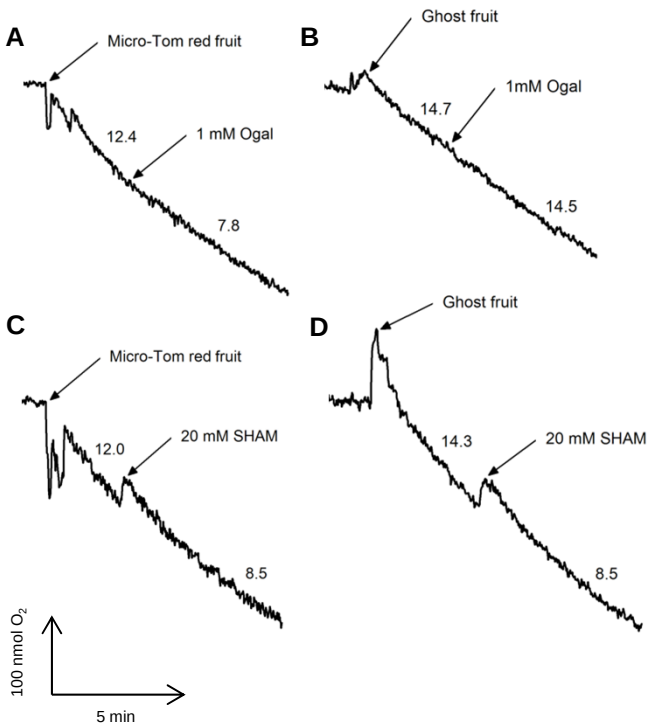

Figure S4. Effect of octyl gallate (Ogal) (A, B) and salicylhydroxamic acid (SHAM) (C, D) on oxygen uptake of ripe tomato fruit pericarp. In traces A and C, Micro-Tom tomato was used. In traces B and D, *ghost* tomato mutant was used. The addition of the inhibitors and their final concentrations in the measurement cuvette are indicated by arrows. Rates are expressed as nmol O_2 kg^{-1} dry weight s^{-1} and were calculated in the linear zone of the oxygen uptake traces. Each experiment was repeated six times, using tissue samples from three different fruits, obtaining similar results.

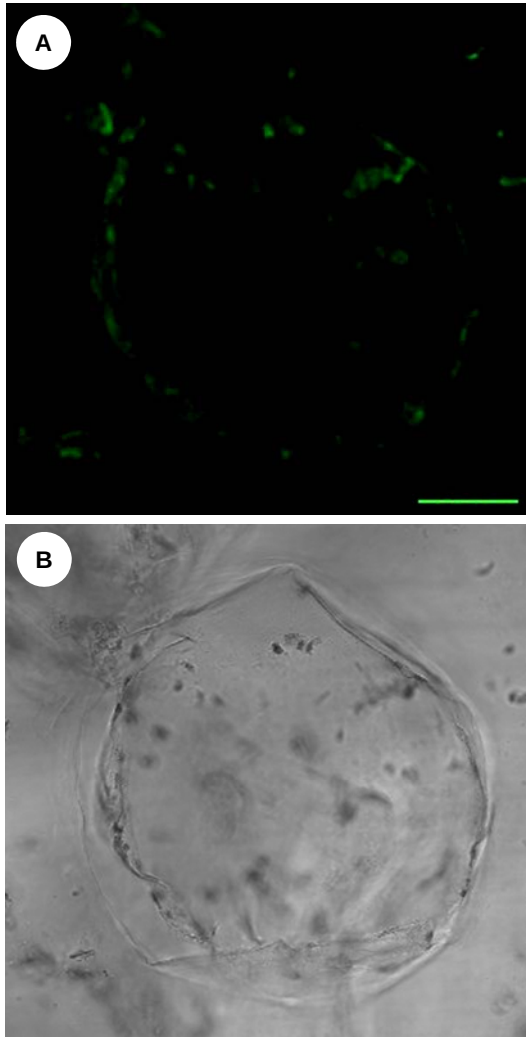

Figure S5. Microscopy images of a pericarp cell from “Micro-Tom” red fruit. A: Confocal image showing the autofluorescence of lycopene (emission: 510-530 nm). B: Corresponding bright field image. Bar (A) = 50 µm.

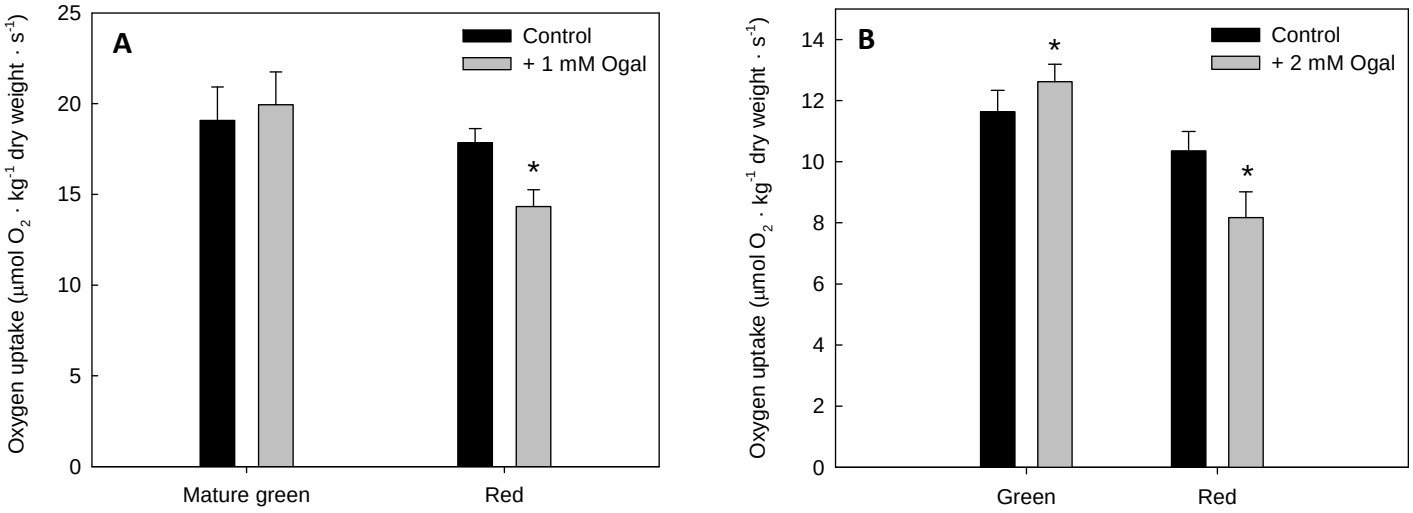

Figure S6. A: Effect of 1 mM octyl gallate (Ogal) on oxygen uptake activity of Ailsa Craig tomato pericarp at mature green and red stages. Data are means of $n = 7 \pm$ SE. Asterisks indicate significant differences from the control (pairwaise *Student's t* test, $P < 0.01$). B: Effect of 2 mM Ogal on oxygen uptake activity of bell pepper pericarp at green (unripe) and red (ripe) stages. Data are means of $n = 4 \pm$ SE. Asterisks indicate significant differences from the control (pairwise *Student's t* test, $P < 0.05$).

	pmol ATP mg $^{-1}$ protein s $^{-1}$				
	Control	**+ CCCP**	**+ Ogal**	**+ DPI**	**+ DBMIB**
NADH	7.1 ± 0.2 *a*	0.5 ± 0.2 *b*	-0.1 ± 0 *b*	4.5 ± 0.4 *c*	5.2 ± 0.9 *c*
NADPH	4.7 ± 0.5 *c*	-0.2 ± 0.2 *b*	-0.2 ± 0.1 *b*	0.4 ± 0.1 *b*	0.5 ± 0.2 *b*

Supplemental Table S1. Effect of 10 µM CCCP, 250 µM octyl gallate (Ogal), 50 µM DPI and 100 µM DBMIB on ATP synthesis activity of Micro-Tom chromoplasts in the presence of NADH or NADPH. The reaction well contained 80 µL of buffer ("Materials and Methods"), 80 µL of luciferase/luciferin reagent, 20 µL of chromoplasts (from 0.08 to 0.14 mg of chromoplastic protein), 20 µM DAPP, 0.1 mM of ADP and 1 mM of NADH (plus 1 mM NAD^+) or 1mM NADPH (plus 1 mM $NADP^+$). Rates are expressed as picomol ATP mg^{-1} protein s^{-1} and were estimated from the slope between 5 and 30 s of the assays. Data are arithmetic means of n = 3 to 4 ± SE. Different letters indicate significant differences (*Student's t* test, $P < 0.05$).

Supplemental Protocol S1. Experimental conditions of the quantitative Real-Time PCR reactions, primer sequences and data from biological replicates.

Reference gene:

Gene symbol	CAC (Clathrin adaptor complex)
Sequence accession number (GenBank/EMBL)	XM_00424491
Primer sequences	Forward: CCTCCGTTGTGATGTAACTGG
	Reverse: ATTGGTGGAAAGTAACATCATCG
Amplicon length (pb)	173
Efficiency	1.805
Standard curve	Slope: 3.898 Y Intercept: 32.17 Error: 0.0147
T_m (melting temperature)	80.1 ± 0.2
C_q [1] of the NTC (No Template Control)	34.8 ± 0.3

Target gene:

Gene symbol	Cytochrome c_6, chloroplastic-like
Sequence accession number (GenBank/EMBL)	XM_004233185
Primer sequences	Forward: TGCACTTTTGGTCCTCGATT
	Reverse: ATCTCTCTCGTCCCATTCGG
Amplicon length (pb)	197
Efficiency	1.708
Standard curve	Slope: -4.301 Y Intercept: 34.78 Error: 0.0185
T_m (melting temperature)	78.4 ± 0.03
C_q [1] of the NTC (No Template Control)	40.0 ± 0.0

Target gene:

Gene symbol	PTOX (Plastidial Terminal Oxidase)
Sequence accession number (GenBank/EMBL)	AF177980
Primer sequences	Forward: ATTTGCCCGCTCCAAAGATT
	Reverse: GGCTCCCGTGAGTTTGACAG
Amplicon length (pb)	195
Efficiency	1.901
Standard curve	Slope: -3.585 Y Intercept: 34.13 Error: 0.059
T_m (melting temperature)	79.79 ± 0.02
C_q [1] of the NTC (No Template Control)	40.0 ± 0.0

[1] C_q: quantification cycle or crossing point.

Materials and methods:

"Micro-Tom" fruits were harvested at small green, mature green, breaker, orange and red stages. Also, the youngest fully-expanded leaves of plants were selected. Tissue was immediately frozen in liquid nitrogen and stored at -80ºC until processed. mRNA extraction was done as described in Bugos et al., 1995, and it was treated with DNase. Next, cDNA was obtained using the Retroscript kit (Ambion, Life Technologies), as recommended by the kit supplier. DNA contamination was excluded by the non-detectable PCR product of non-reverse transcribed mRNA preparations. In order to test the specificity of the primers, cDNA of leaf, mature green fruit and red fruit was used as template in PCR with each primer-pair. A single band with the expected size was obtained for CAC, cytochrome c_6 and PTOX primers.

Real-time amplification reactions were conducted in a LightCycler 480 System (Roche Applied Science) in a 96 multi well-plate, and run in triplicate. The content of each well was: 2.5 µl of 10x diluted cDNA, 5 µl of LightCycler 480 SYBR Green I Master, 1.5 µl of nuclease-free water and 0.5 µM of primers (total volume: 10 µl). NTC (No Template Controls) were run in triplicate for each master mix. To obtain the standard curve and calculate the primer efficiency, a pool of the cDNA of the six different tissues was used as template. The cycling conditions were set as follows: initial denaturation step of 95°C for 10 min to activate the DNA polymerase, followed by 45 cycles of denaturation at 95°C for 10 s, annealing at 60°C for 30 s and extension at 72°C for 30 s. The amplification process was followed by a melting curve analysis, increasing the temperature continuously from 65°C to 95°C.

The quantification cycles or crossing points (C_q) were automatically determined by the LightCycler 480 SW 1.5 software (Second Derivative Maximum Method). The melting curves produced a single peak indicating that a single fragment had been amplified. The differences in mRNA abundance between tomato samples were calculated through normalization with the reference gene CAC, which has been recommended as an exceptionally stable reference gene for suited normalization of different tomato tissues during the complete tomato development process (Expósito-Rodríguez et al., 2008). Small green fruit tissue was set as the calibrator sample and the transcript levels in the rest of the samples are expressed in *n* fold change. The experiment was repeated with three different mRNA obtained in independent extraction processes.

Data from biological replicates:

	Cyt c_6 (A)	Cyt c_6 (B)
Small green fruit	1 ± 0.3	1 ± 0.2
Mature green fruit	0.9 ± 0.3	1.3 ± 0.2
Breaker fruit	1.2 ± 0.2	1.1 ± 0.3
Orange fruit	2.1 ± 0.2	1.8 ± 0.2
Red fruit	1.5 ± 0.3	1.5 ± 0.2

	PTOX (A)	PTOX (B)
Small green fruit	1 ± 0.1	1 ± 0.3
Mature green fruit	2.0 ± 0.1	2.6 ± 0.2
Breaker fruit	6.7 ± 0.2	5.6 ± 0.2
Orange fruit	7.7 ± 0.4	13.3 ± 0.2
Red fruit	7.3 ± 0.2	5.8 ± 0.2
Leaf	0.7 ± 0.1	0.7± 0.2

Literature cited:

Bugos RC, Chiang VL, Zhang XH, Campbell ER, Podila GK, Campbell WH (1995) RNA isolation from plant tissues recalcitrant to extraction in guanidine. Biotechniques **19**: 734–737

Expósito-Rodríguez M, Borges AA, Borges-Pérez A, Pérez JA (2008) Selection of internal control genes for quantitative real-time RT-PCR studies during tomato development process. BMC Plant Biol **8**: 131